POLITECNICO DI TORINO

Corso di Laurea Magistrale in Ingegneria Biomedica

Master Thesis

High-Density surface EMG for the investigation of myotonic discharges in subjects with myotonic dystrophy

Advisors:
Prof. Marco Gazzoni
Eng. Alberto Botter
Dr. Elda Judica

Candidate:
Enrica Tricomi

Academic year 2018/2019

To my Parents,
for giving me roots and wings.

Acknowledgements

I would like to thank Casa di Cura Privata del Policlinico and, particularly, my supervisor Dr. Elda Judica and Dr. Peppino Tropea for their professionalism, availability and help throughout the realization of the present work.

I am sincerely thankful to my advisors, Marco Gazzoni and Alberto Botter, for the constant help and teachings, but also for the guidance and the wise and precious pieces of advice. I would like to thank Giacinto Luigi Cerone for all the support, valuable suggestions and technical help. I am grateful to all the LISiN members for giving me the opportunity to take part to this family for a while.

I would like to thank my Mother and my Father, my greatest source of inner strength in dealing with hard challenges, those who have always encouraged me to go after my dreams even when the mountains where too hard to climb, those who have always been by my side and made all of this possible.

I am thankful to my little sister Virginia and my little brother Pietro, for always showing me that family is a safe haven, for all the hard times in which their presence and hugs cheered me up during these years, for all their love I can't live without. I love you both more than anything.

I would like to thank my loving grandmother Tina, for the unconditional love she shows me every single day, for her concern every time I was worried, for taking care of me every day since I was born teaching me valuable life tricks that let me become the person I am today.

I am grateful to all my uncles, aunts, and cousins for all the support and care.

Last, but definitely not least, the biggest of all thanks to my love, Salvuccio, who always encourages me to explore and go beyond my limits, who sustained me throughout everything, from whom I learned that barriers are made to be overcome, from whom I learned to never give up, and to whom I owe all of this. No words would ever be enough.

Summary

Myotonic dystrophy is a rare and slowly progressive neuromuscular disorder caused by genetic defects. To date, two forms of myotonic dystrophy have been identified: myotonic dystrophy type 1 (DM1 or Steinert's disease) and myotonic dystrophy type 2 (DM2 or PROMM). Myotonic dystrophy is characterized by progressive myopathy, muscle weakness, multiorgan failure involvement, and myotonia. Myotonia can be defined as excessive and prolonged muscle excitability and muscle contraction at rest, right after muscle percussion or at the end of the excitatory stimulus. It is possible to identify two forms of myotonia: clinical myotonia that consists in incomplete relaxation of muscle following either voluntary contraction or direct percussion, and electric myotonia that is an abnormal muscle fibre membrane electrical activity observed by needle EMG examination.

Nowadays, needle electromyography is the gold standard to confirm the presence of myotonic discharges. Nevertheless, due to its invasiveness and limited detection volume, needle Electromyography (EMG) present a number of drawbacks. The present study, conducted in collaboration with Casa di Cura Privata del Poliniclico di Milano, proposes to objectively characterize the phenomenon of myotonia in a population of patients affected by myotonic dystrophy in a non-invasive manner by means of the so-called High-Density Surface Electromyography (HDsEMG). This technique allows studying in a non-invasive way the peripheral and central properties of the neuromuscular system. The main aims are: a) to assess the involvement of specific muscles or muscle compartments of the forearm during myotonic discharges, b) to investigate motor units' characteristics and recruitment in pathological and healthy patients.

Six patients with myotonic dystrophy and eight healthy controls underwent experimental examination. HDsEMG and force signals were acquired by means of a 96-electrode grid overlying the forearm flexor muscles of the subject's dominant hand and a handgrip dynamometer. According to the clinical tests used to elicit myotonic contractions, we studied EMG activity during and after hand closing. The subject was requested to perform three sets of contractions with 10-minute interval of rest between them. Each set consisted of 6 maximal voluntary isometric contractions, each lasting 3 seconds, with a 10-second rest period in between.

Signals were processed to assess muscle activity, muscle recruitment and motor units behaviour. Firstly, some indexes were extracted from the force signals, such as the relaxation time (indicating the time required for decline in force from 90% to 10% of the peak force after each contraction) and rise time (the time taken for the rising edge of the force profile to go from 10% to 90% of the maximum). Secondly, global muscle activity behaviour was studied through the application of an algorithm for the detection of activation and deactivation instants. In the end, the single motor unit templates and discharge patterns were extracted through an automated signal decomposition algorithm to gain insights into the central properties of motor control. The relaxation time identified over the descending phase of the force profile was correlated with the muscle relaxation time estimated from muscle on-off timing. A statistical analysis was then performed to assess whether the patients' and controls' rise and relaxation times were statistically significant different.

From the analysis of the mechanical output, patients showed lower levels of muscle strength in concordance with the data coming from clinical examinations. Patients were characterized by longer relaxation times, although no statistically significant different from the controls'. Muscle activation and deactivation pattern followed the rising and falling edges of the force profile in the control group, while patients' data were characterized by a high variability. Particularly, two patients, who reported the feeling of myotonia after muscle contractions, showed prolonged muscle activation pattern with respect to the descending phase of the force profile. The time required by muscles to relax (extracted from the on-off timing) and the relaxation time extracted from the mechanical output resulted highly correlated. In two of six patients HDsEMG decomposition brought to the identification of a delayed de-recruitment of some motor units.

With this study an experimental setup was defined to study myotonia through HDsEMG. Signal decomposition results showed a slow de-recruitment of some motor units at the end of the contraction in two of four patients that reported the subjective feeling of myotonic discharges. Given the limited number of patients under analysis, it is not possible to reach conclusions on the potentials of the proposed technique. However, preliminary results support the idea that HDsEMG may contribute to the characterization and the study of myotonia. Further validations are necessary to assess the possibility of generalization on a larger sample.

Table of Contents

List of Acronyms

BMI	Body Mass Index
CAR	Common Average Reference
CKC	Convolution Kernel Compensation
CM	Clinical myotonia
CNS	Central Nervous System
CWT	Continuous Wavelet Transform
DM1	Myotonic dystrophy Type 1
DM2	Myotonic dystrophy Type 2
EMG	Electromyography
EM	Electric myotonia
HDsEMG	High-Density Surface Electromyography
NDD	Normal Double Differentiating filter (Laplace filter)
MVC	Maximal Voluntary Contraction
MEACS	Miniaturized EMG Acquisition System
MD	Myotonic dystrophy
MIRS	Muscular Impairment Rating Scale

MU	Motor Unit
MUAP	Motor Unit Action Potential
MUAPTs	Motor Unit Action Potential Trains
PNR	Pulse-to-Noise Ratio
RMS	Root Mean Square
SD	Single Differential filter
sEMG	Surface Electromyography

Chapter 1

Introduction

1.1 Myotonic dystrophy (MD)

Myotonic dystrophy (MD) is one of the most complex pathologies ever known. It is a rare and slowly progressive genetic disorder that affects the neuromuscular system. It is inherited in a dominant pattern and with the worsening of symptoms in each generation [1]. Main symptoms are progressive myopathy, muscle loss, myotonia (delayed relaxation after muscle contraction), muscle weakness, and multiorgan failure involvement.

Up to the present, two forms of MD have been identified:

- *Myotonic Dystrophy Type 1* (DM1 or Steinert's disease);
- *Myotonic Dystrophy Type 2* (DM2 or PROMM).

Although these two conditions present similar symptoms, they also have a variety of different features. Noteworthy differences between the two forms of MD include the pattern of muscle weakness, systemic features, age of onset, the limited evidence of central nervous system involvement in DM2, and the absence of congenital cases in DM2 [2]. Therefore, they are considered as two separate diseases [3] (Table 1.1). In both cases, the disorder affects the single muscle fibres causing an increased variation in fibre diameter that ranges from 10 μm to more than 100 μm and the presence of a high number of central nuclei [4]. To date, there is no specific treatment neither

for DM1 nor for DM2. The only chance is to focus on managing the complications of the disease.

1.1.1 Myotonic dystrophy Type 1 (DM1)

Myotonic dystrophy Type 1 (DM1) was the first form of MD discovered and it is referred to as the classic form of MD. It was first described by Steinert and colleagues in 1909, hence the name Steinert's disease [3]. It is the most frequent form of muscular dystrophy with adult onset (with a worldwide prevalence of 1/8000) [5], and it is inherited with anticipation and increasing severity in successive generations [6]. The genetic defect that brings to this kind of MD was discovered later, in 1992, and was found to be an unstable expanded CTG triplet repeat on chromosome 19 [7]. The affected gene is the DMPK, a gene that codes for a protein expressed in skeletal muscles, the myotonic dystrophy protein kinase [3].

DM1 can be classified into four types according to clinical manifestations, severity, and age at onset [8]:

- The *congenital form* may appear in newborns of mothers affected by MD. This form brings to respiratory and feeding problems, hypotonic cerebral palsy, and mild to moderate cognitive disability in those who survive;
- The *childhood form* brings to learning disability and mild or absent neuromuscular signs at onset;
- The *typical form* has onset in adolescence or early adult life and it is characterized by severe impairment of the neuromuscular system;
- The *mild form* has onset in middle or older age and it is characterized by minimal muscular or no symptoms;

In DM1, the first muscles to be damaged by the pathology are the distal ones, such as finger flexors and intrinsic hand-muscles, leading to the impairment of hand function [1]. Proximal muscles become involved with the progression of the disease. Muscle weakness can lead to complications including scoliosis, contractures [5], and foot drop in the case of weakness of ankle dorsiflexion [2]. Main features are grip and percussion myotonia, even though myotonia can affect also other muscle such

as tongue, bulbar, or facial muscles bringing to chewing, talking, and swallowing problems [3].

1.1.2 Myotonic dystrophy Type 2 (DM2)

Myotonic dystrophy Type 2 (DM2) is an autosomal-dominant systemic disease that was discovered only in the second half of the '90s. Although very similar to classic myotonic dystrophy, DM2 present some different features. The differences between the two forms can be found in the genetic defect and in muscle impairment. As for the genetic basis, DM2 was found to be a tetranucleotide repeat disorder rather than a trinucleotide repeat disorder. More in details, it is caused by an unstable CCTG tetra-repeat expansion in ZNF9/CNBP gene on chromosome 3 [7].

In this second form of MD the limb-muscle weakness affects often more proximal muscles than distal ones and muscle atrophy is less. For this reason, DM2 form was initially referred to as proximal myotonic myopathy (PROMM), or proximal myotonic dystrophy (PMD). Muscle weakness in DM2 involves deep finger, thumb flexors, neck muscles, and hip and elbow extensors [2].

	DM1	**DM2**
Age of onset	0 to adult	8-60
Life expectancy	Reduced	Normal range
Anticipation	Always present	Exceptional
Muscle weakness	Distal muscles	Proximal muscles
EMG myotonia	Present	Absent or variable
Clinical myotonia	Evident in adult onset	Present in <50%
Cataracts	Present	Present in minority
Dysphagia	Present in later stages	Absent
Respiratory muscles weakness	Present in later stages	Unusual
Tremors	Absent	Present in many
Cognitive disorders	Present	Not apparent
Cardiac arrhythmias	Present	From absent to severe
Diabetes	Frequent	Infrequent

Table 1.1: Main features and clinical manifestations of DM1 and DM2 [3].

1.1.3 Myotonia in MD

Myotonia can be defined as excessive and prolonged muscle excitability and muscle contraction [9] at rest, right after percussion or at the end of the excitatory stimulus. This symptom is a feature of myopathies, a group of neuromuscular disorders primarily affecting the single muscle fibre and the structures of its supportive connective tissue. Generally, among all the myopathies, myotonia is found in the myotonic dystrophies (type 1 and type 2) and in the non-dystrophic myotonias (such as hyperkalemic periodic paralysis, paramyotonia congenita, and myotonia congenita) [10]. The pattern of affected muscles vary depending on the specific disorder.

Myotonia is the result of an increased excitability of the muscle membrane caused by ion channels dysfunction. In details, in the specific case of myotonic dystrophies, chloride and potassium conductance is found to be normal, while alterations were found in sodium channels reactivations. Specifically, during the inactivation process, the sodium gates spontaneously reopen generating additional inward sodium current depolarizing again the muscle membrane. Repetitions of this process result in a sustained muscle contraction lasting for some time generating the observed myotonic discharges [11]. For this reason, myotonia is mainly treated with drugs that act as antagonists of the reopening of sodium channels, such as mexiletine, that reduce muscle action potential, but muscle power as well [9] [10].

It is possible to distinguish two forms of myotonia:

- *Clinical myotonia (CM)* consists in not complete relaxation of muscles following either direct percussion or voluntary contraction. Usually it appears trying to relax handgrip or after muscle percussion using a reflex hammer. While grip myotonia is not always present, percussion myotonia is nearly always demonstrable, above all by percussion of the thenar eminence [2]. In other words, it can be defined as delayed relaxation of skeletal muscles resulting in muscle pain and stiffness [6].

- *Electric myotonia (EM)* is the result of the abnormal muscle fibre membrane electrical activity [2] and it appears as repetitive muscle fibre potential discharges that wax and wane in frequency and amplitude [7] with a firing rate between 20 and 80 Hz [6]. This form of myotonia is observed on needle EMG

examination.

Among all the myopathies, MD is characterized by both EM and CM, even though myotonia may not necessarily affect every muscle. Furthermore, since muscle weakness often predominates in proximal muscles in DM2, it might be supposed that myotonic discharges would be more prominent proximally in this form. On the contrary, in DM1 myotonic discharges and weakness might be supposed to be distally predominant [7]. One remarkable feature is the worsening of myotonia with a lower ambient temperature and during the first muscle contraction. Repeated contractions can improve the myotonic phenomenon bringing to an easier relaxation of the muscles, the so called "warm-up phenomenon" [11].

1.2 Assessment of the disorder

1.2.1 Needle Electromyography (EMG)

Nowadays, the presence of MD is best confirmed by DNA analysis. Nevertheless, electromyography is still important in the evaluation of the pathology [12]. Besides, since myotonia may not show on clinical examination, needle electromyography is still the gold standard to confirm the presence of myotonic discharges. This is especially the case for DM2 patients in whom percussion and grip myotonia may be absent or undetectable [6].

Electromyographic potentials can be recorded with needle electrodes inserted in a muscle and derive from the action potentials of single muscle fibres firing near the electrode [13] (Figure 1.1). All voluntary contractions are mediated by motor neurons and the muscle fibres innervated by the axonal branches (a complex referred to as Motor Unit (MU)). The sum of electric potentials of the muscle fibres belonging to a MU is the so-called Motor Unit Action Potential (MUAP) [14].

Needle electromyographic examinations represent to date the gold standard in clinics for the identification of electrical activity for its high spatial selectivity [15] and the possibility to investigate MUAP morphology, duration, amplitude, and recruitment. Indeed, electric signals are accurately represented thanks to the closeness of the needle electrode to single motor units [16]. Thus, this technique suits well for

the detection of abnormalities in motor unit size and internal structure. In addition, this technique allows the investigation of motor units at the peripheral and at the central level. At the peripheral level, it allows to study diseases affecting the single muscle fibres (myopathies, such as muscular dystrophies), the ability of the nerve to regenerate (reinnervation), the effects of lesions (e.g., denervation), and diseases of the neuromuscular junction. At the central level, it allows to study the firing patterns and recruitment of MUs [17]. However, depending on the type of electrodes used, the recorded MUAP can be the sum of action potentials from a different number of muscle fibres and from muscle fibres in different locations [13] [17] .

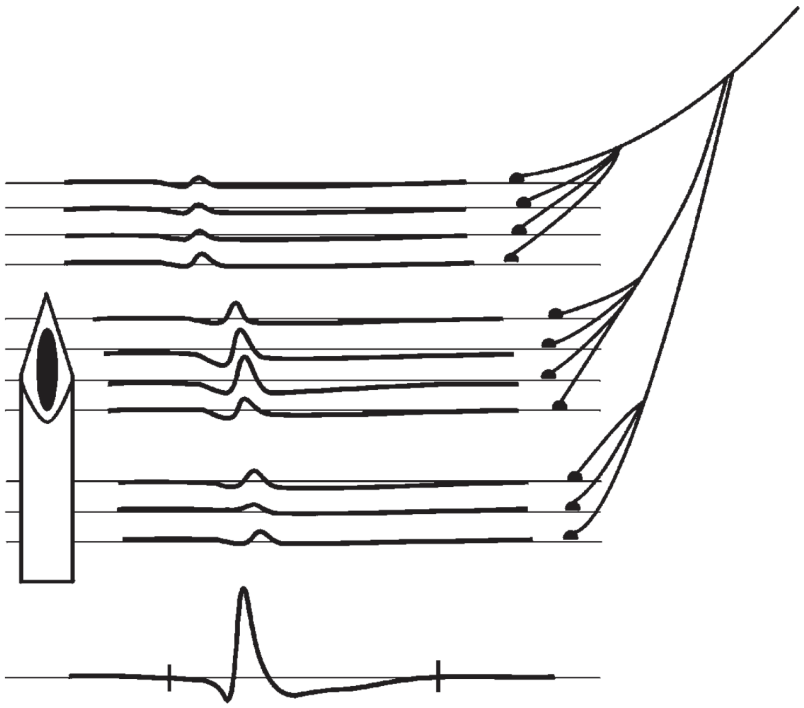

Figure 1.1: Detection of MUAP by a concentric needle electrode. The action potentials that are recorded with higher amplitude are the ones of muscle fibers closest to the recording electrode [17].

Despite its advantages, needle EMG has also several disadvantages related to its invasiveness. First of all, it has limitations related to the painful procedure and to the impossibility to be performed in those cases when needle insertion is not advisable or not possible (e.g., clinical examinations of children, professional athletes, patients

with transplanted limbs, and, in general, dynamic conditions) [15]. In addition, when performed, each muscle may require separate needle insertion sites to detect subtle abnormalities [11] bringing to the destruction of several muscle fibres [18]. Other limitations are related to the small measurement area and the dependence of signal amplitude on the position of a few muscle fibres near the needle tip. All of this brings to a lack of reproducibility of needle EMG measurements [19].

Motor Unit and MUAP morphology changes in MD

The MUAP is normally recorded with a triphasic configuration, given the propagation of the action potentials toward and then away from the recording electrode. The morphology of each MUAP can be described in terms of amplitude, number of phases, rise time, and duration (Figure 1.2). In absence of pathological states, normal MUAPs last 8–10 ms and have firing rates of 5–8 Hz that increase up to 20 – 40 Hz as the effort increases [13] (normal recruitment). In neuromuscular diseases, MUAP characteristics may be altered.

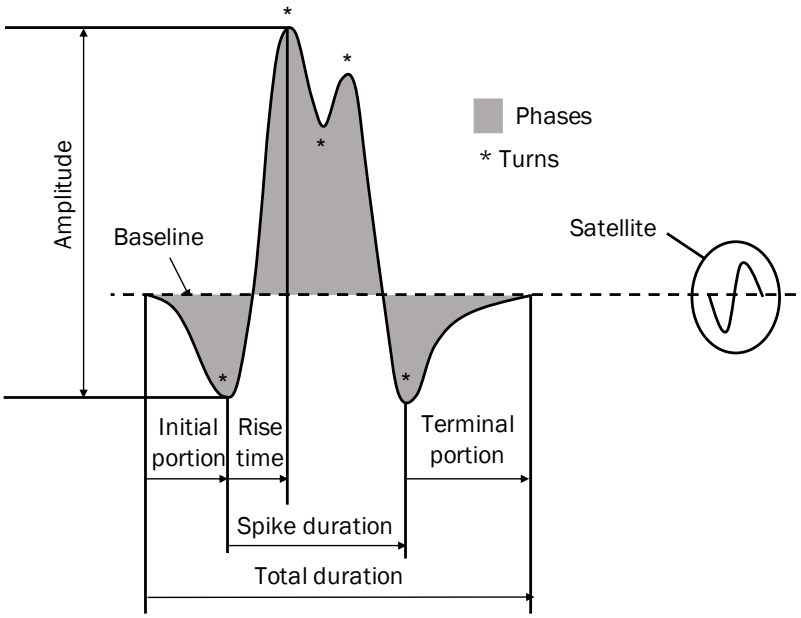

Figure 1.2: Schematic representation of a single MUAP waveform.

With reference to myopathic disorders, the number of available motor units does

not change, but the size of the MU decreases as a consequence of a dropout or dysfunction of individual muscle fibres (Figure 1.3). This results in short, small and polyphasic MUAPs, sometimes referred to as myopathic unit. In particular, the decrease of the duration can be related to the decrease of the total number of muscle fibres in each motor unit [20]. Another characteristic is an early recruitment pattern, meaning that with increasing force of contraction motor units progressive recruitment is anticipated [21]. Being motor units smaller than normal, they can generate only smaller amount of force than normal conditions. For this reason, subjects need to recruit many MUAPs even when producing low force levels. The result is an interference pattern with many units firing at the same time but producing little power [20] [21].

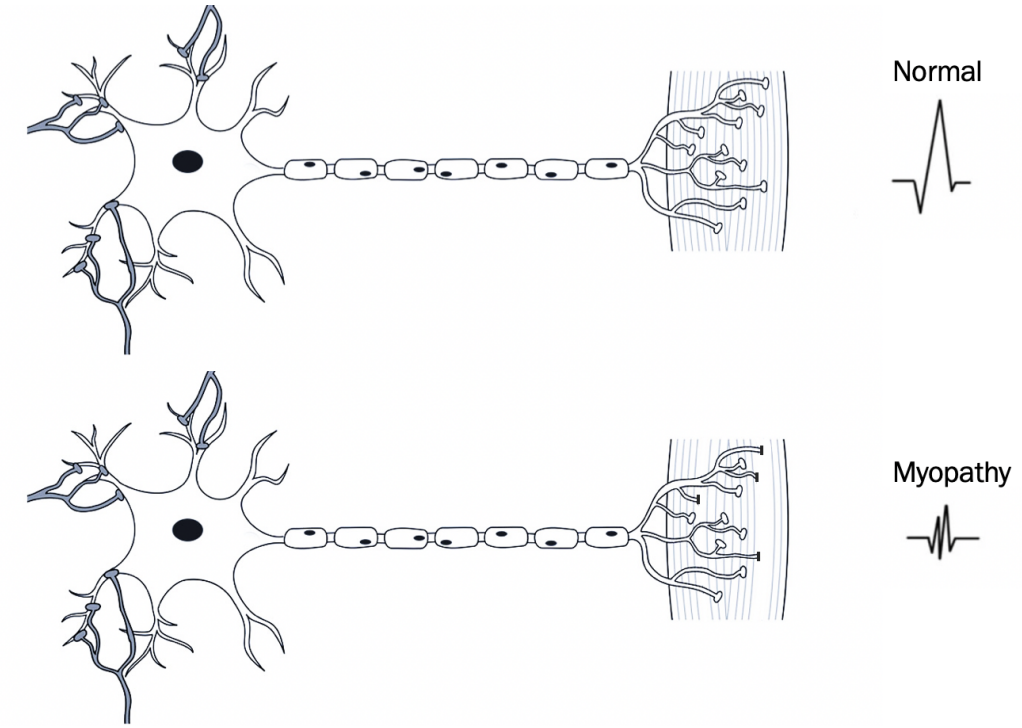

Figure 1.3: Physiologic model of motor units in myopathies. The number of available motor units does not change, but the size of the MU decreases as a consequence of a dropout or dysfunction of individual muscle fibres. Consequently, each MUAP is generated by fewer motor fibres resulting in polyphasic, short, and low in amplitude.

Myotonic discharges detected by needle EMG

Myotonic discharges are the action potentials of single muscle fibres that keep firing spontaneously after excitation. These potentials appear because of an abnormality in the membrane of the muscle fibre and wax and wane in amplitude and frequency [13], with firing rates that vary between 40 and 100 Hz [6].

According to previous studies investigating myotonic discharges with needle EMG technique [7], it seems that the features of EM are different in the two forms of MD. Indeed, in DM2 patients only a less specific waning pattern without a waxing component was observed [22] (Figure 1.4).

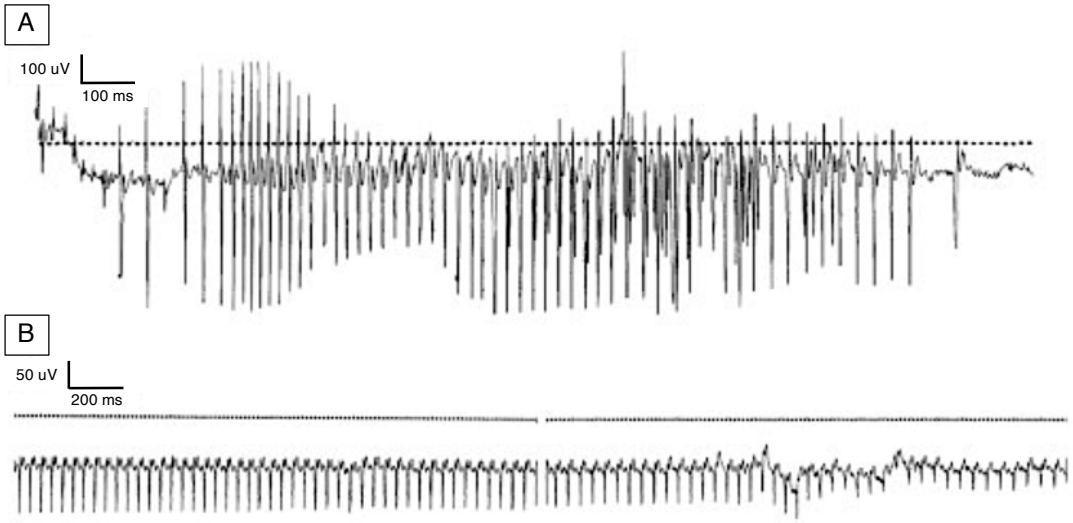

Figure 1.4: EM (A). Two-second myotonic discharge in a DM1 patient. The typical waxing and waning pattern in frequency and amplitude can be noted; maximal frequency about 60 Hz, minimal about 8 Hz. (B). Four-second myotonic discharge in a DM2 patient in which frequency and amplitude gradually decline without waxing component; maximal frequency toward onset about 23 Hz, minimal toward termination about 19 Hz. [7]

Myotonic discharges have different appearance if elicited by the insertion of the needle or whether they occur after voluntary contraction. In both cases, both amplitude and frequency wax and wane as the discharge continues. When elicited by the insertion of the needle, myotonic potentials appear as positive waves, with an

initial sharp positivity followed by a negative component of long duration, while myotonic discharges that occur after a voluntary contraction are similar to fibrillation potentials, being initially positive and brief, biphasic or triphasic spikes. This afterdischarge corresponds to the poor relaxation that is clinically evident, referred to as CM [13]. Myotonic discharges may occur with or without the presence of CM, even though when CM is present, the myotonic discharges are often prominent and frequent [13].

1.3 High-Density Surface Electromyography

Surface Electromyography (sEMG) is a non-invasive technique to measure muscle activity by means of surface electrodes placed over the skin [16]. This technique provides information on muscle fatigue and on the temporal activation and deactivation pattern of muscles. For this reason, it suits best in studies investigating movement analysis, in sport sciences, in rehabilitation research, and ergonomics [18]. sEMG is also used for diagnostic purposes, especially in patients with neuromuscular disorders, since the procedure is less painful than needle electromyography [16].

Nevertheless, when recorded with the classic bipolar montage, sEMG amplitude information is highly influenced by the localization of the recording electrodes. In addition, bipolar recordings are characterized by inappropriate representation of muscle activity whether the pick-up volume does not allow the collection of signals from representative amounts of the active motor units, lacks of selectivity, and problems related to crosstalk based on the chosen inter-electrode distance. These factors may limit the amount of physiological information that can be extracted by sEMG recordings [23]. In particular, the poor selectivity of bipolar sEMG systems [24] brings to the representation of muscle activity only from a global point of view, ignoring its spatio-temporal behaviour.

With the development of High-Density Surface Electromyography (HDsEMG), a technique that use multiple closely spaced electrodes overlying a muscle or a group of muscles [14] [16], it became possible to sample the muscular electrical activity over a larger surface area [25] and to extract information at the single MU level. The recording and processing of sEMG signals in a two dimensional space can overcome

some of the limits of single-channel approaches, allowing the quantification of the spatial and temporal properties of the electrical muscle activity [26]. Furthermore, using grids of electrodes, the selectivity of the system increases and each MUAP is represented as a spatio-temporal profile of the corresponding MU [27]. All of this allows the study of more detailed information, such as the location of the innervation zone, the mapping of the MUAP propagation from the innervation zone to the tendons, the estimation of muscle-fibre conduction velocity, as well as length and orientation of the fibres [17] [24]. Moreover, if the grid is aligned with the direction of the muscle fibres, the spatial distribution of the potential maintains a similar shape during propagation [25]. With needle EMG it is not as easy to investigate this MU properties, thus, sEMG may provide information related to the physiological or pathological states of the neuromuscular system [24]. To some extent, HDsEMG recordings allow also the investigation of recruitment and the decomposition of the signal into constituent motor unit action potential trains [28] through the help of automated signal decomposition algorithms [15]. An example of HDsEMG signal is provided in figure 1.5.

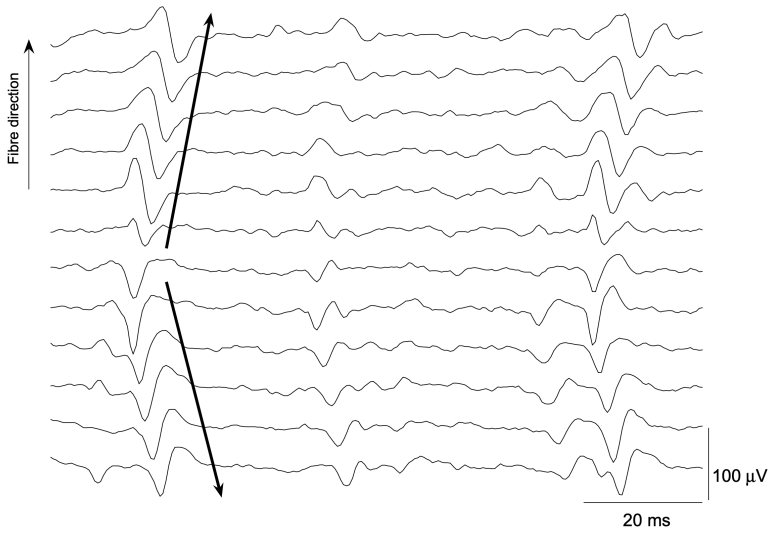

Figure 1.5: Motor unit action potentials in a electrode array placed over the biceps brachii. The bipolar derivation is shown. It is possible to detect the motor endplate zone identified by the low amplitude and the reversal of signal polarity. From the innervation zone the MUAPs propagate along the fibre towards the tendons [14].

When using grids composed by multiple electrodes, one important aspect relies on the electrode-skin contact impedances that must be low, stable over time and similar from one electrode to another [25]. Indeed, it is required an appropriate and accurate preparation of the skin. To these purposes, the design of electrode grids has been progressively improved bringing to flexible printed circuit technology where electrodes are embedded in flexible silicon rubber. These grids allow a more stable electrode-skin contact by means of adhesive foam interposed between the skin and the grid with holes filled with conductive gel [25].

With respect to needle EMG, with surface electrodes the distance and the tissue interposed between the skin and muscle fibres act as a filter decreasing the high-frequency components of the EMG signal and, as a consequence, the amplitude. This inherent problem has limited sEMG diagnostic applicability. Nevertheless, the development of analysis of spatio-temporal information provided by grids of electrodes has increased the applicability of the surface EMG method [12].

The different EMG techniques and their target of investigation are schematically represented in Figure 1.6.

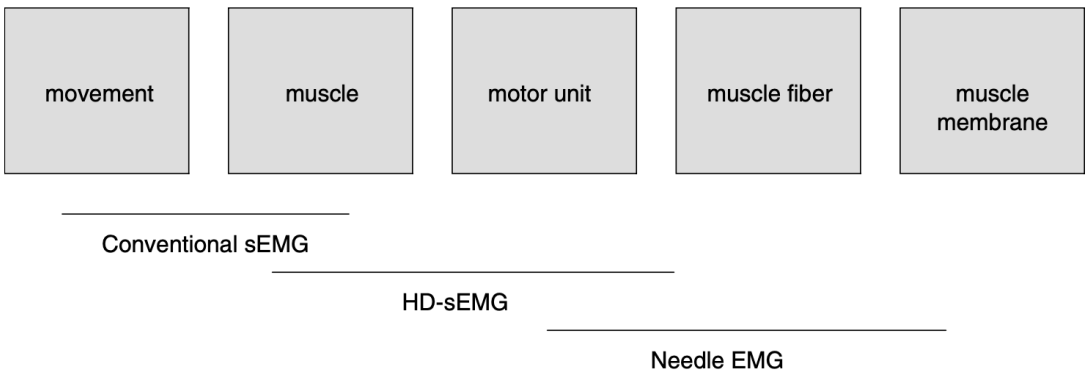

Figure 1.6: The target of the different EMG techniques. Conventional bipolar sEMG is mainly used in movement analysis. HDsEMG technique provides information on muscle–fibre conduction velocity and can be used to supplement the information obtained with needle electrodes at the muscle–fibre level [16].

1.4 Aims of the study

Up until now, while handgrip strength and the delayed relaxation caused by myotonia in patients with MD has been well documented [29][30], it was not developed a satisfactory method of documenting and analysing myotonic discharges during grip myotonia through non-invasive techniques. In particular, to our knowledge, no study focused on the analysis of both the electrophysiological features and mechanical manifestations of grip myotonia.

The only previous attempt to observe handgrip myotonia in MD by means of surface electromyography was that of Torres, Moxley, and Griggs (1983) [29]. This study focused both on measures of the relaxation times through the use of an handgrip dynamometer and on the observation of myotonia from the long flexors of the fingers through skin surface electrodes. The authors focused on the measurement of relaxation time, maximum voluntary contraction time, and fatigue time (Figure 1.7). In particular, relaxation time was studied as a mean of quantification of clinical myotonia. Torres et al. noticed a remarkable reduction of the Maximal Voluntary Contraction (MVC) in all patients, especially in those with more severe distal weakness on clinical evaluation. Moreover, relaxation time resulted to be markedly prolonged in all patients compared to normals. In particular, in the myotonic dystrophy group they noticed a flattening of the curve in correspondence of the point where the falling edge of the relaxation curve met the baseline. As for the electromyographic recordings, in myotonic dystrophy the amplitude of the sEMG signal was found to be smaller than in normals. The authors observed a wide variability in the myotonic phenomenon.

Even though the aforementioned study investigated the phenomenon of myotonia in a non-invasive way combining force measures with sEMG recordings, the authors did not explore the electrophysiological features of grip myotonia analysing the single channel sEMG trace. Moreover, they limited to quantify grip myotonia only by means of relaxation times curves from the force profile.

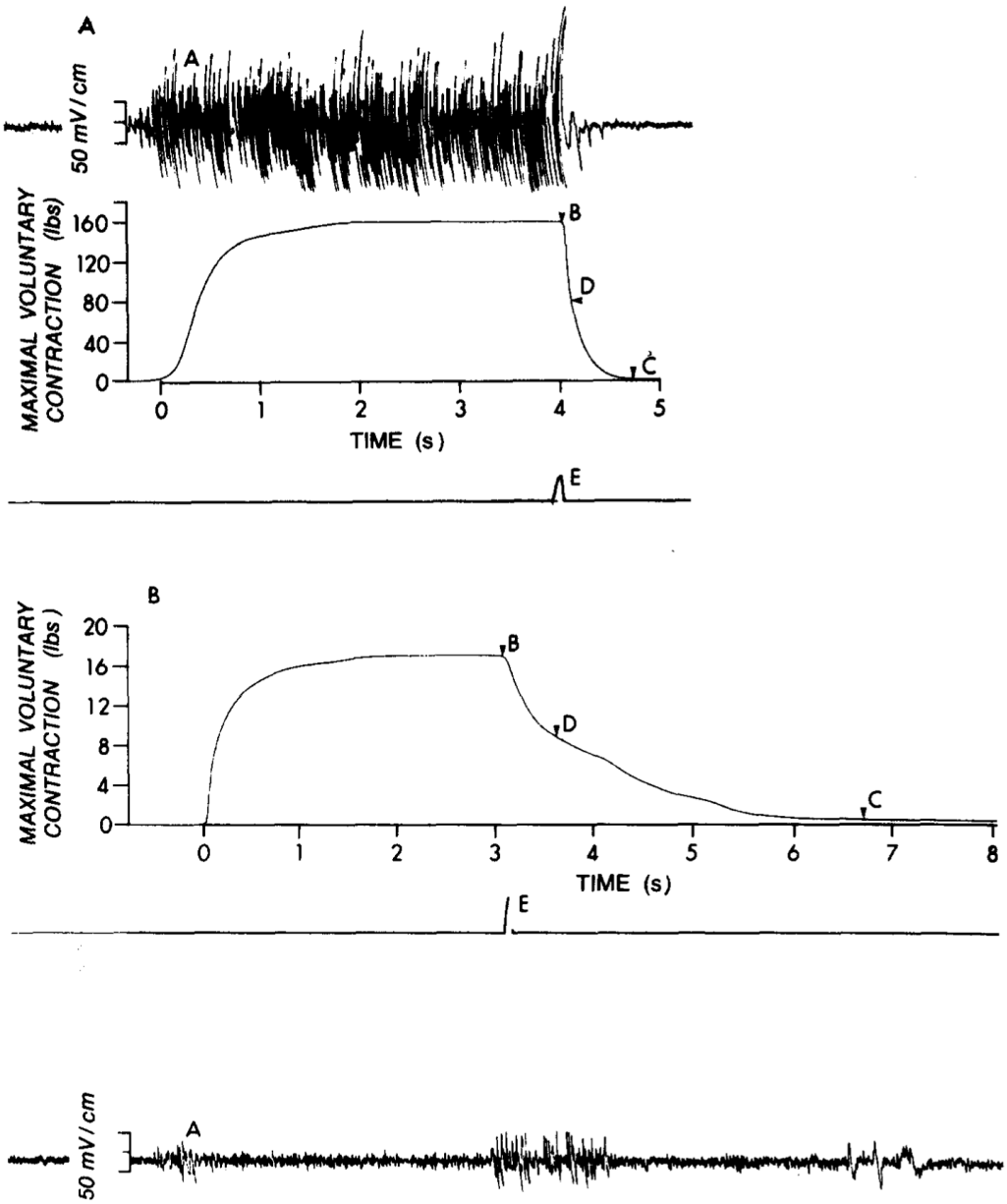

Figure 1.7: Torres et al. (A) EMG recorded by surface electrodes from the grip long flexors. The figure on the top displays the trace of a normal subject and the one on the bottom the one of a myotonic dystrophy patient. (B) The tension force curve reaches its maximum that is sustained until the onset of relaxation. (C) The point where the falling curve meets baseline measures the 100 RT. (D) RT 50 [29]

With the purpose of examining the myotonic phenomenon during handgrip, the present study, conducted in collaboration with Casa di Cura Privata del Policlinico, proposes objective and non-invasive methods to investigate the electrophysiological and mechanical features of grip myotonia in MD. With this study, we propose the investigation of grip myotonia in MD by means of a grid of electrodes covering the all forearm flexors area (the so-called HDsEMG technique), and to correlate it with the measure of grip muscle strength and force profile during a series of isometric contractions, as well as with clinical and genetic data. To our knowledge, this is the first study to evaluate together muscular activation parameters (e.g., Root Mean Square (RMS), HDsEMG activation maps) and intensity/severity of the myotonic phenomenon parameters (e.g., relaxation time, presence and intensity of myotonic discharges).

An innovative experimental setup and HDsEMG processing techniques are proposed in order to achieve a primary and a secondary goal.

Primary goal

As a primary goal, this study aims to objectively investigate the phenomenon of myotonia in a population of patients affected by MD (DM1 and DM2) of different features: gender, pathology age of onset, and the assumption or not of mexiletine. In particular:

- it aims to assess the involvement of specific muscles or muscle portions of the dominant upper limb with the use of HDsEMG technique during and after handgrip.
- it aims to investigate MU pattern characteristics and recruitment through decomposition of sEMG signals in pathological and healthy subjects;
- it aims to investigate the correlations between clinical evaluations and the quantitative variables coming from HDsEMG;

Secondary goal

This study aims to compare mechanical and sEMG variables extracted from patients affected by MD with the data extracted from the group of healthy controls.

1.4.1 Hypothesis

In this study, we hypothesized that the non-invasive evaluation of muscle activity through HDsEMG may allow the assessment of muscles and muscle compartments involved in the myotonic afterdischarge during handgrip, as well as the abnormal motor units' recruitment pattern.

The main expectations concerned results that allows to outline a non-invasive experimental setup and objective experimental protocol to characterize the phenomenon of myotonia, both in view of a targeted upper limb rehabilitation and in view of a modulation of the pharmacological treatment.

To sum up, this research study aims both to explore the clinical applicability of HDsEMG in the investigation of the phenomenon of myotonia in patients with MD, as well as to obtain pathophysiological insights.

Chapter 2

Preliminary study: identification of the optimal detection system

In this chapter, a preliminary study is presented with the purpose to gain insights on the forearm flexors activation during tasks involving hands and wrist movements. This preliminary analysis aimed at spatially localize the EMG amplitude distributions of flexor muscles for the assessment of the most active portions during specific tasks. During this phase, a detection system covering the most of the skin area over the flexors was used. The final goal was to assess the optimal detection system for the recording of the electrophysiological activity during handgrip based on the localized active areas. This preliminary investigation was carried on following the methodology described by Gallina and Botter [23].

2.1 Muscles under investigation

Being grip myotonia the focus of the main study, the muscles under investigation are the ones in the anterior compartment of the forearm which perform wrist and fingers flexion and pronation. These muscles are organized into three layers: superficial, intermediate, and deep. A brief description of the superficial muscles of the ventral compartment of the forearm is provided in the following.

Flexor Carpi Ulnaris
The Flexor Carpi Ulnaris muscle (or FCU) acts to flex and adduct (medial deviation) the wrist joint. It arises by two heads, humeral and ulnar. It passes into the wrist, and attaches to the pisiform carpal bone.

Palmaris Longus
The Palmaris Longus (or PL) performs wrist flexion. It originates from the medial epicondyle and attaches to the flexor retinaculum of the wrist. It is absent in about 14 percent of the population. However, the absence of this muscle does not have an effect on grip strength.

Flexor Carpi Radialis
The Flexor Carpi Radialis (or FCR) performs flexion and radial abduction of the wrist. It originates from the medial epicondyle, attaches to the flexor retinaculum of the wrist and runs just laterally of flexor digitorum superficialis.

Pronator Teres
The Pronator Teres (or PT) serves for the pronation of the forearm. It has two heads – humeral and ulnar. The muscle passes obliquely across the forearm, and ends in a flat tendon.

Flexor Digitorum Superficialis
The Flexor Digitorum Superficialis (or FDS) is the only muscle belonging to the intermediate compartment, although it can sometimes be classified as a superficial muscle. It performs the flexion of the wrist, of the metacarpophalangeal joints, and proximal interphalangeal joints at the four fingers.

A sketch of the anatomy of the muscles under investigation is provided in Figure 2.1.

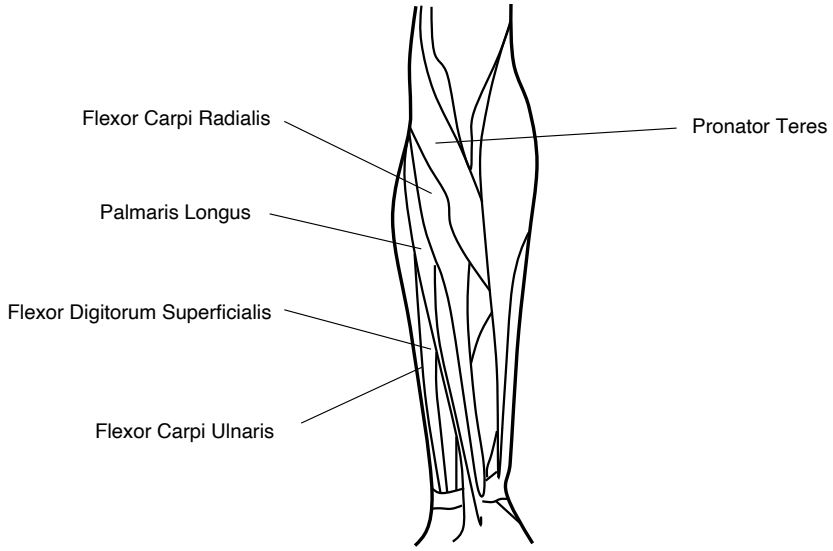

Figure 2.1: Anatomy of the investigated muscles of the ventral compartment of the forearm. In the superficial layer: the Pronator Teres pronates the forearm, the Flexor Carpi Radialis, the Palmaris Longus, and the Flexor Carpi Ulnaris deal with the wrist motor control. In the intermediate layer: the Flexor digitorum superficialis deals with finger flexion.

2.2 Experimental setup and Protocol

Six healthy subjects were tested (three females and three males, age: 25±2 years, weight: 61±12 kg, height: 170±10 cm). All subjects reported no upper limb pathologies. The detection system consisted of three bi-dimensional electrode grids composed of 32 Ag electrodes equally spaced by 10 mm in rows and columns. The three grids were organized to form a unique electrode grid of 96 electrodes in 12 rows and 8 columns. Before placing the electrode grid, a line was drawn between the point of insertion of the distal biceps tendon and the radial styloid process. The length and proximal circumference of the forearm were measured. The length of the forearm was considered equal to the length of the line, the circumference of the forearm was measured at 1/3 of the length of the line starting from the distal biceps' tendon insertion. The grid was then placed aligning the first column with the line, and the first row at 3 cm from the point corresponding to the distal biceps tendon insertion (see Figure 2.2). The grid was placed on the right forearm of the subject.

This electrodes configuration was chosen to cover approximately the overall area of the ventral forearm. Despite that, some muscles at the edges of the grid may be not completely represented in some subjects, being the dimension of the forearm different from one subject to another [23].

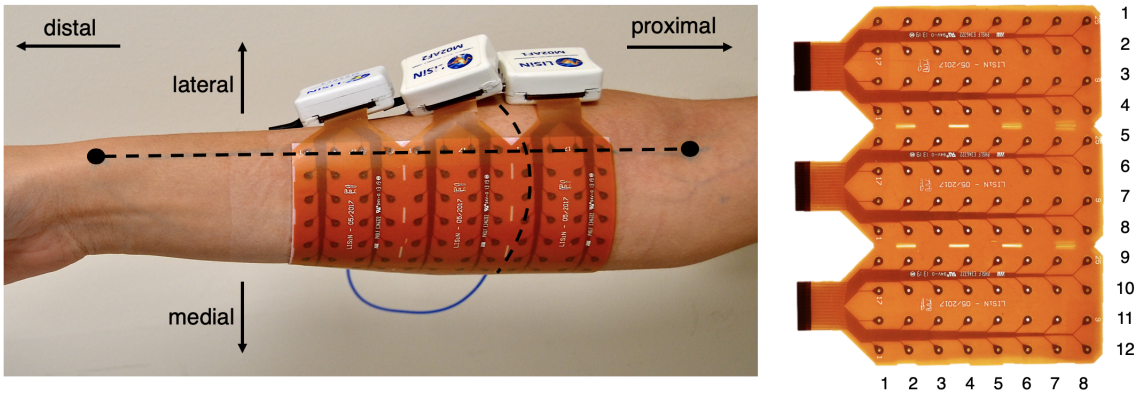

Figure 2.2: The detection system consisting of three bi-dimensional grids (LISiN, Politecnico di Torino) organised in a unique grid of 12 rows and 8 columns. The first column was aligned with the line linking the point on the distal biceps tendon and the one over the radial styloid process. The first row was placed at 3 cm from the point on the distal biceps tendon.

In order to localize the main areas of activation of the forearm flexors while performing wrist and hand motor control, the subjects were asked to perform the following isometric contractions:

- *Wrist flexion*: the subjects were asked to perform wrist flexion while the wrist was kept in a fixed position. In this case the muscles involved in the movement are the flexor carpi ulnaris and the flexor carpi radialis.

- *Pressing little, ring, middle and index fingers against the thumb*: the subjects were asked to press the fingers one by one against the thumb as much as possible while maintaining the other fingers relaxed and the wrist in a fixed position. In this case, the muscle activation involves the flexor digitorum superficialis, activating different portions of the muscle while changing the finger.

- *Hand kept as a fist grasping a rigid cylindric object*: the subjects were asked

to grasp an object while keeping the wrist in a fixed position to activate the finger flexors.

- *Hand kept as a fist grasping a soft cylindric object*

Contractions were registered for 5 seconds. During the contractions, the forearm was kept at about 120° flexion and the wrist in mid-pronation. The subject was asked to maintain this position throughout the duration of the experiment.

2.3 Data acquisition and processing

sEMG signals were collected through miniaturized wireless and modular acquisition systems for HDsEMG (Miniaturized EMG Acquisition System (MEACS), LISiN, Politecnico di Torino). Each acquisition system performs the conditioning, sampling, and wireless transmission of 32 monopolar sEMG signals, sampled at 2048 samples/s with 16 bit resolution. Each electrode grid was connected to an acquisition system, and the three systems were connected to a single reference electrode placed over the elbow (Figure 2.3).

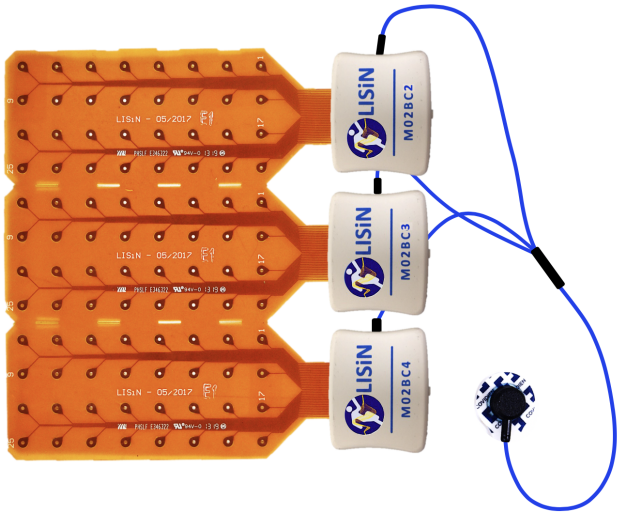

Figure 2.3: The three miniaturized wireless and modular acquisition systems for HDsEMG (LISiN, Politecnico di Torino) connected to the three grids and to a unique reference electrode. The acquisition systems perform the conditioning, sampling at 2048 Hz and wireless transmission of data.

For each subject and each task, the signals collected from the three grids were passband filtered between 20 Hz and 400 Hz with a Butterworth filter of order 4 and organized in 12 rows and 8 columns for the visualization. Signal quality was assessed through visual analysis in the time domain, and bad channels were replaced using a linear interpolation of the neighbours. Because of the not perfect acquisition synchronism among the three systems during the acquisitions, the signals of the three grids had to be realigned. The alignment process is described in Chapter 3 in details. An example of monopolar signals from a representative subject is shown in fig. 2.4.

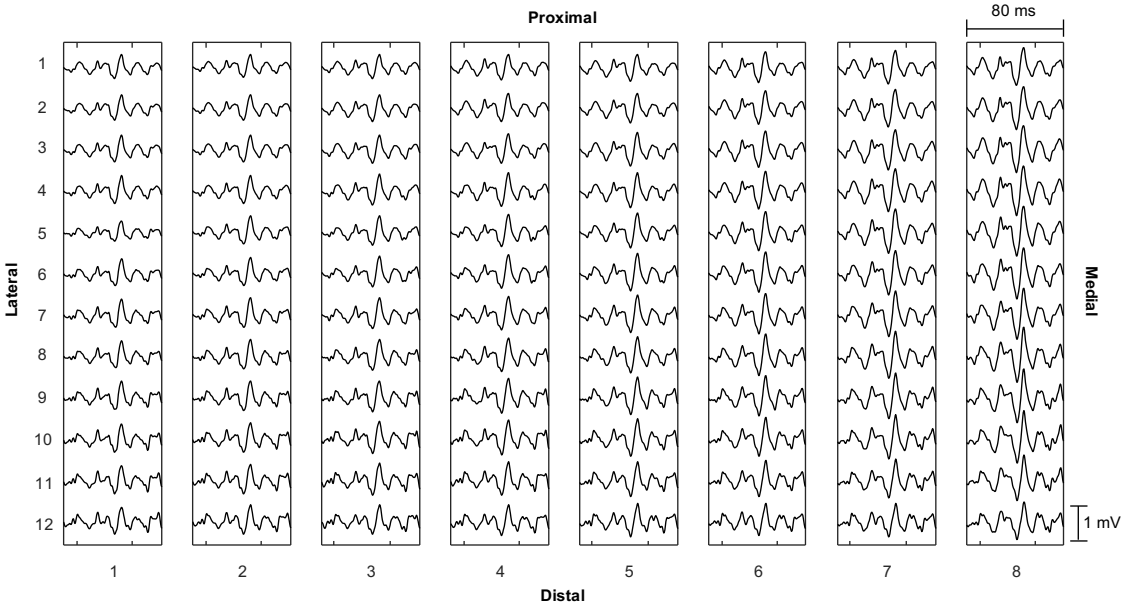

Figure 2.4: 80 ms epoch of the signals collected from S1 during the task "Little finger pressed against thumb". As expected, the largest MUAPs are observed in the medial portion of the grid (contraction of Flexor Digitorum Superficialis).

To localize the barycentre of muscle activation over the electrode grid during the performed tasks, the monopolar amplitude distribution of the sEMG signal was obtained computing the RMS of each channel of the grid during a 1-second signal epoch in the middle of the contraction (seconds: 2-3). For the barycentre computation, the channels with an RMS value higher than 70% of the maximum RMS value were identified. The barycentre was then computed weighting the RMS values of the

identified channels with the respective coordinates over the grid. Lastly, the position of the barycentre was normalized with respect to the anatomical measures of the subjects (length and proximal circumference of the forearm) and used to define the location of the active area.

2.4 Results

The average forearm length was 24 ± 1,3 cm (mean ± standard deviation), whereas the proximal forearm circumference was 21,1 ± 7,5 cm. Examples of colour maps and barycentre identification from a representative subject are shown in figure 2.5.

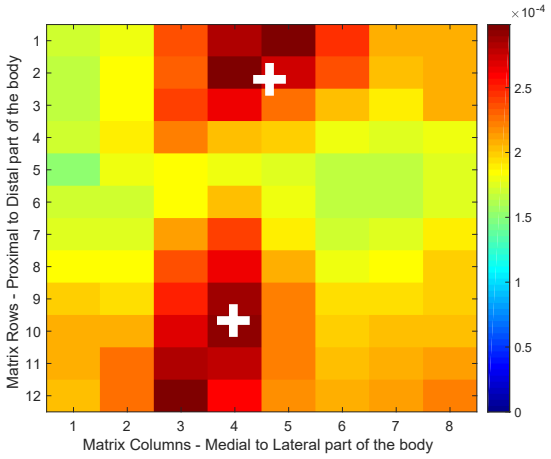

S1, Wrist Flexion

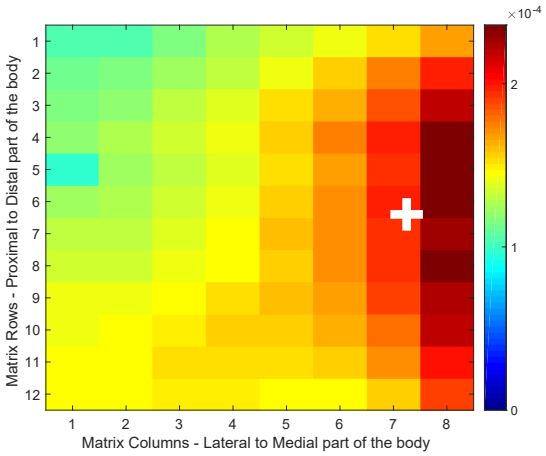

S1, Little finger against the thumb.

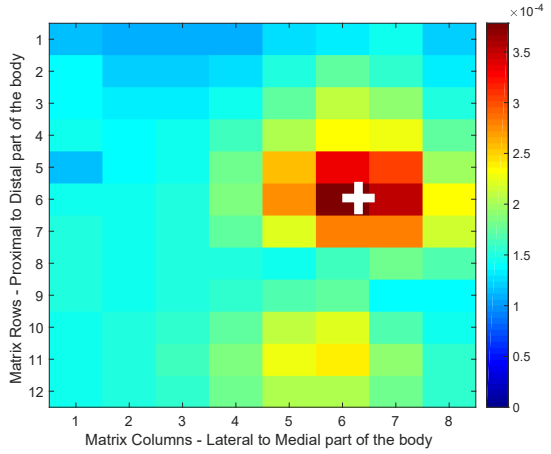

S1, Ring finger against the thumb.

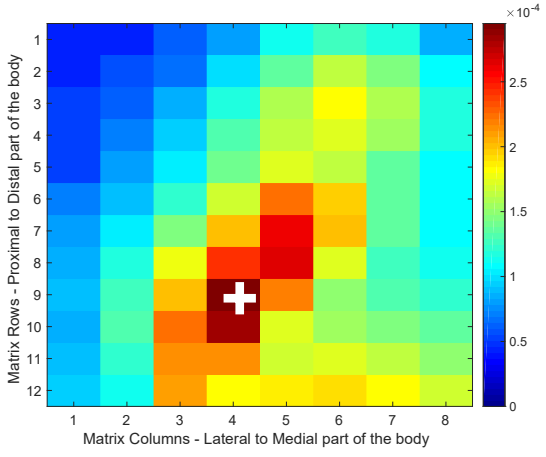

S1, Middle finger against the thumb.

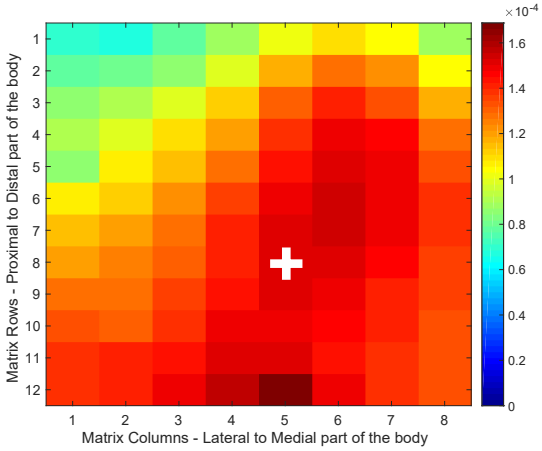

S1, Index finger against the thumb.

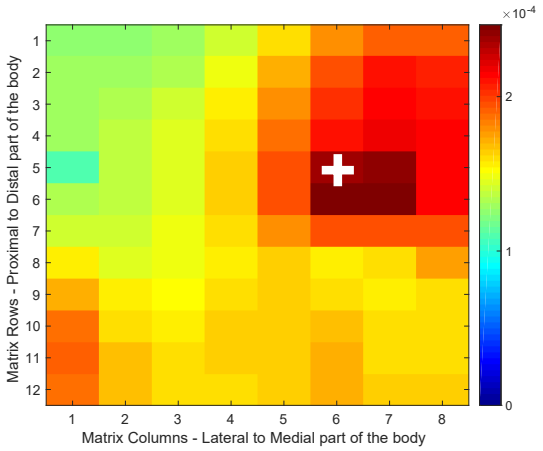

S1, Hand as a fist grasping a rigid cylindric object .

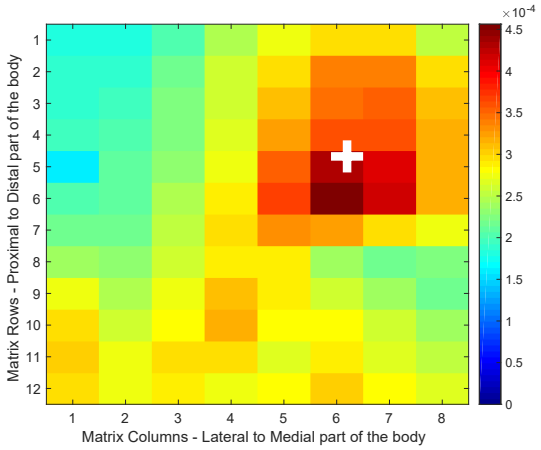

S1, Hand as a fist grasping a soft cylindric object.

Figure 2.5: sEMG amplitude distributions (RMS) over the forearm during the seven tasks of a representative subject (S1). The colour bar ranges from zero (blue) to the peak of amplitude (in Volts) of the map (red). The white cross represents the barycentre of the channels that overcome the threshold of the 70% of the maximum RMS value.

Considering the channels with an RMS value higher than the 70% of the maximum RMS value, almost every task showed only one cluster of activation. Only the task "Wrist Flexion" showed more than one cluster. In this case, since different clusters could represent different muscles, a barycentre for each cluster was computed, so as

not to consider the portion in the middle of the clusters as the centre of activation.

In order to make a comparison among the subjects for the same task, the barycentre was normalized with respect to the anatomical measures of all subjects. The X coordinate of the barycentre (Eq. 2.1) was normalized with respect to the forearm circumference, and the Y coordinate (Eq. 2.2) was normalized with respect to the length of the forearm. For the Y coordinate it was considered that the grid was placed at 3 cm from the insertion point of the distal tendon of the biceps muscle. The positions of the mean clusters' barycentre of the six subjects are represented in Figure 2.6 subdivided by task.

$$X_{coord} = \frac{Bar_x}{circ} 100 \tag{2.1}$$

$$Y_{coord} = \frac{Bar_y + 3}{length} 100 \tag{2.2}$$

Analysing the results, it is possible to assert that the monopolar EMG amplitude distributions of the activity of contracting muscles in the forearm area allow the discrimination of different contractions [23]. In this case, except for the task "Wrist Flexion", the centres of activation range more or less between 30% and 60% of the forearm length. Consequently, it was evaluated the possibility to exclude one of the three grids and to place the remaining ones over the identified region. Nevertheless, considering that the barycentre is a piece of punctual information, the mean barycentre of the six subjects could not always be considered as representative of the active areas for every subject. Indeed, placing the threshold at the 70% of the maximum RMS value, in some tasks, approximately all the channels of the matrix overcame the threshold. Thus, relying only upon the mean barycentre and the range, active muscles and portions of the forearm would be excluded whenever the setup would be simplified. For this reason, other tests were driven to further validate the simplification of the setup from three grids to two.

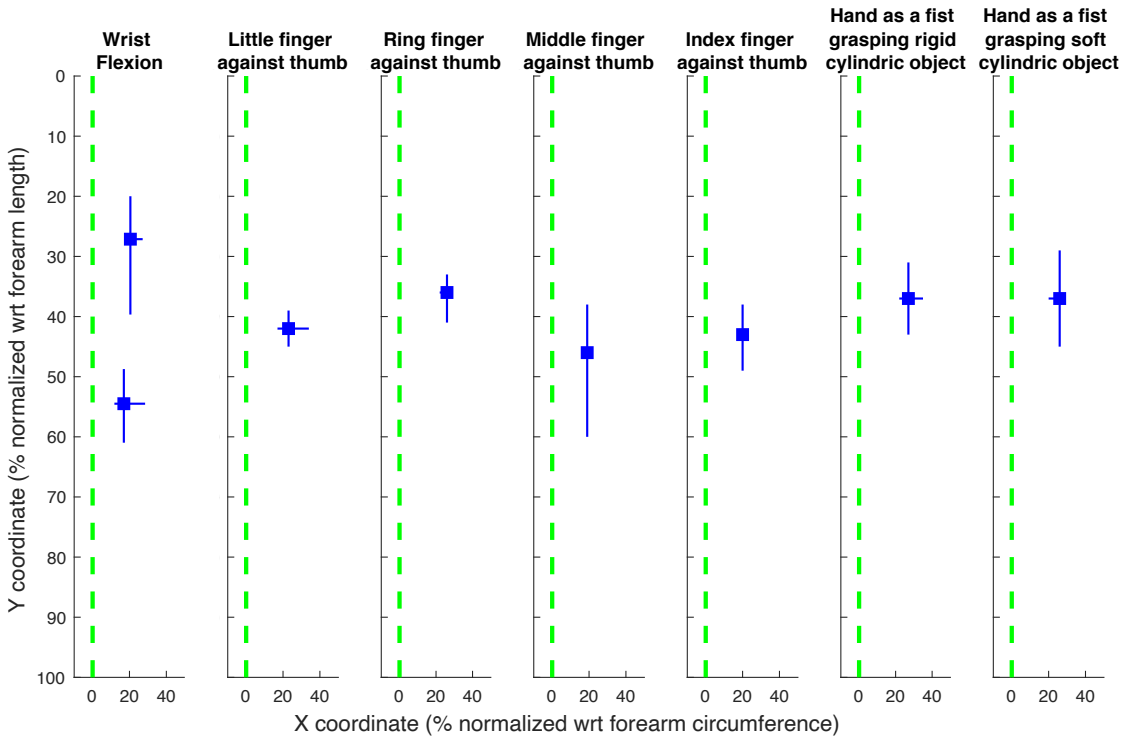

Figure 2.6: Mean barycentre of all subjects represented by the square and the range represented by vertical and horizontal lines. The y axis represents the length of the forearm considering the 0% the point of insertion of the distal biceps tendon and 100% the radius styloid process. The x axis represents the circumference of the forearm. The x coordinate was normalized with respect to the forearm circumference, and the y coordinate was normalized with respect to the forearm length. The green, dashed line represents the line linking the point on the distal biceps' tendon and the one over the radius styloid process.

The contour lines of the clusters of activation were extracted in order to understand if the barycentre could be considered as representative of the whole active area. The contour lines of the clusters from a representative subject are provided in Figure 2.7. As expected, in relation with the defined threshold, in some cases (see the tasks Little finger and Index finger against the thumb) almost all the channels are considered as active, making the narrow zone identified by the barycentre not so representative of the active region.

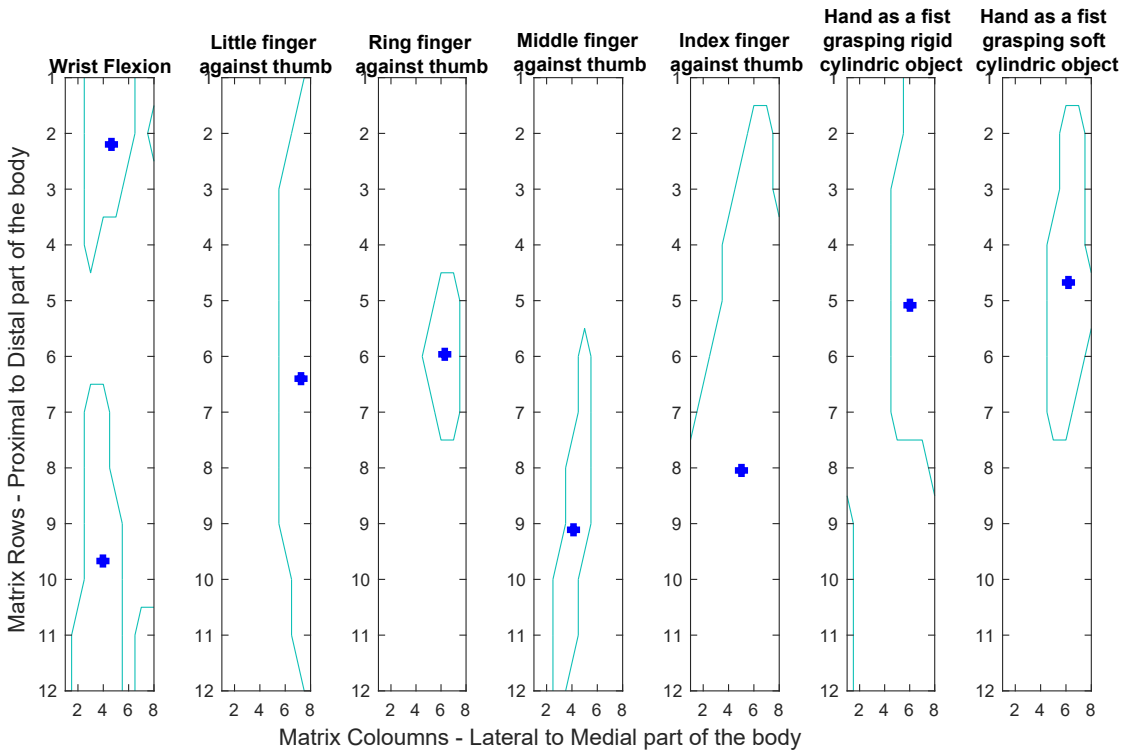

Figure 2.7: Clusters' contour lines and clusters' barycentre from a representative subject (S1) for every task. For most of the tasks, only one cluster was identified. For some of the tasks, the identified clusters extend for a sizeable area of the whole electrode grid.

To conclude, considering only the mean barycentre and the range as reliable data, important information regarding the EMG amplitude distributions of forearm muscles during hand and wrist motor control could be lost. For this reason, the three electrodes grids configuration was considered the optimal detection system to adequately sample the forearm flexors activation and, thus, it was adopted for the main study.

Chapter 3

Materials and methods

In this chapter the materials and methods of the study are introduced. Firstly, patients recruitment criteria and the experimental procedure are presented. Secondly, the off-line data processing and the different methods for the data analysis are described.

3.1 Experimental protocol

The present study was approved by the ethic committee of Casa di Cura Privata del Policlinico di Milano.

3.1.1 Patients selection

Eight patients with MD (four males and four females, age: 45 $\pm$ 13 years) were recruited through Casa di Cura Privata del Policlinico. Three patients were under pharmacological anti-myotonic treatment with mexiletine, while the other five patients were not. In seven of the eight patients was diagnosed Type 1 form (DM1), while one was diagnosed Type 2 form (DM2). The healthy volunteers (six males and four females, age: 38 $\pm$ 14 years) were recruited among the staff members of Casa di Cura Privata del Policlinico and LISiN research centre, trying to match their age and gender with respect to patients as much as possible. The controls did not have any history of neuromuscular disorders. Both patients and controls signed an informed consent for the participation to the experimental study.

Patients were selected according to some inclusion and exclusion criteria.

Inclusion criteria:

- Age >18 years;
- Diagnosis of Myotonic dystrophy (MD) (both forms are taken into consideration) through DNA analysis;
- Presence of clinically evocable myotonia in the upper limb;
- MMSE (Mini-Mental State Examination) >24;

Exclusion criteria:

- Refuse or inability to sign the informed consent;
- Visual acuity deficit;
- Dominant upper limb orthopaedic pathologies;
- Upper limb amputation;
- Other severe clinical problems;

3.1.2 Force recordings

To record the force profile and measure grip strength throughout each contraction, an handgrip dynamometer was designed. With this purpose, a literature research was necessary to find out about the range of forces covered by the human hand during grip. According to literature studies [31] [32], human hands in normals can exert up to more than 500 N. Thus, the choice of the force transducer relapsed on a load cell with a linear voltage output over a force range from 0 to 100 kgf (0-988N), sensitivity of 2.0±1 % mV/V, and cell dynamic of 3.3 V (DaCell Load Cell). In the end, the handgrip dynamometer was composed by the aforementioned force transducer attached to a metal plate and connected to an handle. The metal plate was covered by a soft surface conformed to the shape of the hand and forearm. Velcro stripes were added to keep the forearm firm to the metal plate (Figure 3.1).

Figure 3.1: Handgrip dynamometer composed of a force transducer attached to a metal plate and connected to an handle.

Force signals were recorded by the DueBio probe (OT Bioelettronica, Turin), a modular wireless system designed to acquire biomechanical signals at 2048 Hz with 16 bit resolution and to transmit data wirelessly to a pc through Bluetooth connection (Figure 3.2). Squeezing the handle attached to the load cell, the force signal was displayed in real-time on a PC monitor and stored for off-line analysis.

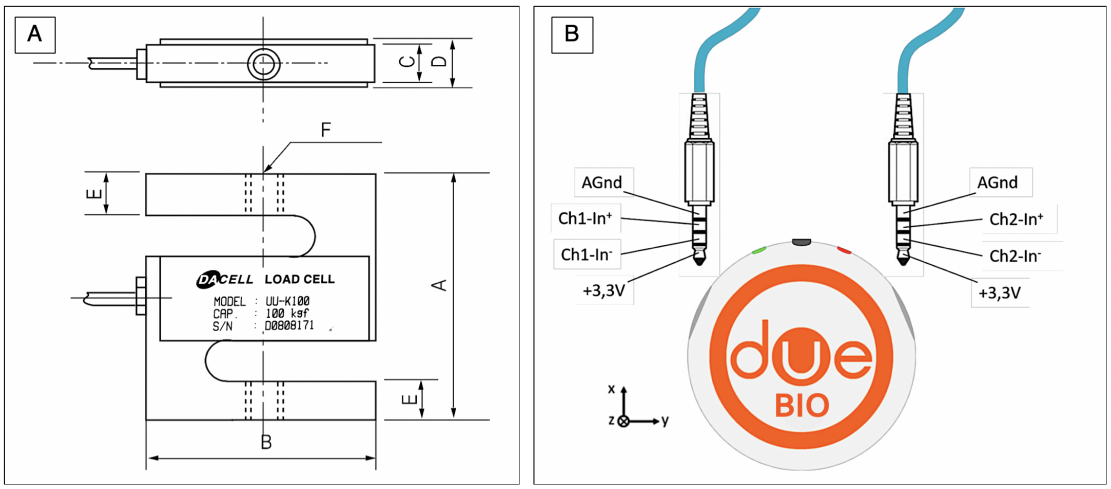

Figure 3.2: **A.** Load Cell (DaCell Load Cell) with a linear voltage output over a force range from 0 to 100 kgf (0-988N), sensitivity of 2.0±1 % mV/V and cell dynamic of 3.3 V. **B.** DueBio probe, a modular system designed to acquire biomechanical signal at 2048 Hz with 16 bit resolution and to transmit data via Bluetooth to a pc.

3.1.3 sEMG recordings

Electrophysiological activity was recorded through a detection system composed of a 12x8 Ag electrode grid placed over the ventral compartment of the forearm following the same positioning described in the preliminary study discussed in Chapter 2. HDsEMG signals were acquired in monopolar configuration by means of the three miniaturized acquisition systems described in Chapter 2 (MEACS, LISiN, Politecnico di Torino) at 2048 Hz with 16 bit resolution. The three acquisition systems were connected to a unique reference electrode placed over the subject's elbow. The skin was accurately scrubbed before applying the electrode grid.

3.1.4 Description of the motor task

The subject's dominant hand was used for testing. Subjects seated in a chair and the handgrip dynamometer was placed on a table. The forearm was fixed in horizontal position and mid-pronation over the metal plate of the handgrip dynamometer at about 120 degrees flexion (Figure 3.3). The hand was kept free, but the subject was asked to keep the fingers on the handle of the dynamometer throughout the duration of each set of contractions to eliminate the use of finger and wrist extensors during the relaxation phase. Indeed, a complete relaxation of the hand and fingers muscles can be achieved even without full extension of the fingers during grip [29].

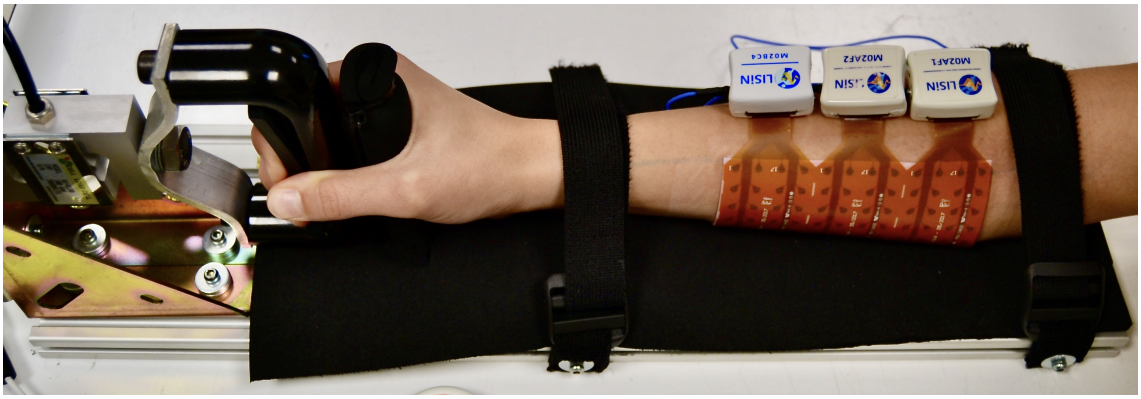

Figure 3.3: Subject's dominant hand was used for testing. The hand was free and the forearm was fixed in horizontal position and in mid-pronation over the metal plate of the handgrip dynamometer at about 120 degrees flexion.

According to the clinical tests used to elicit myotonic contractions, the subject was requested to perform three sets of contractions with 10-minute interval of rest between them. Each set consisted of 6 maximal voluntary isometric contractions, each lasting 3 seconds, with a 10-second rest period in between. The subject was asked to release the grip as fast as he/she could after each MVC contraction. Before and during each contraction verbal encouragement was provided to patients.

During the motor task, a visual and audio feedback was provided to the subject on a PC monitor (Figure 3.4). The audio feedback was needed to scan the contraction times and rest times, while the visual feedback was provided to motivate subjects to reach the targeted force during each contraction. Being the subject's MVC the desired target, a calibration procedure was necessary before each set of contractions to set the requested level of force on the visual feedback screen. For the calibration procedure subjects were asked to squeeze the handle of the dynamometer as hard as they could for few seconds to record the peak force, automatically set as the target by the acquisition software. The provided visual feedback consisted then in a screen with two rows of bars: the upper set of bars (the target bars) allowed the selection of the targeted force level after calibration (the right extremity was set to the subject's MVC, while the other bars referred to decreasing percentages of the MVC from right to left); the lower set of bars (the signal bars) referred to the force level reached by the subjects while squeezing the handgrip dynamometer. The force exerted during an MVC contraction taken from each subject during the calibration procedure was used to trace the ideal force profile (3 seconds of maximal voluntary contraction and 10 seconds of rest) and superimposed to the real force profile.

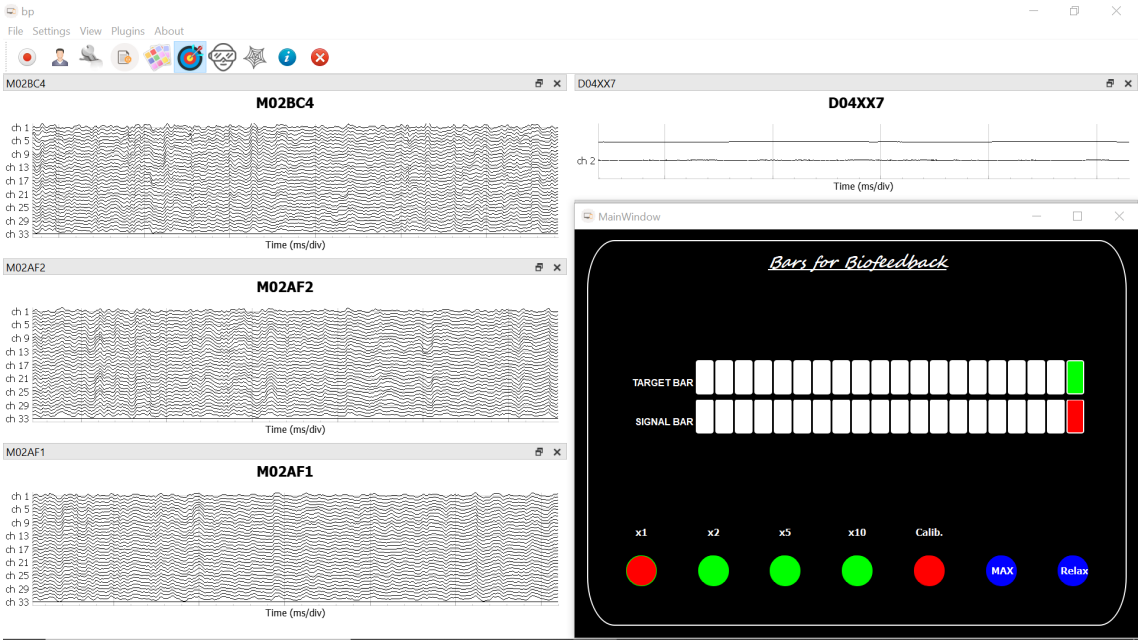

Figure 3.4: The HDsEMG signals (on the left) and force signal (on the right upper portion) during a maximal voluntary contraction. Visual and audio feedbacks were provided to subjects during the trials. The target of the visual feedback was set to the subjects' MVC (marked in green on the visual feedback screen). Squeezing the handle of the dynamometer, the signal bar (marked in red) moved forward and backward according to the subjects' exerted force.

3.2 Data processing

3.2.1 Force signal processing

Force signals were low-pass filtered with a Butterworth filter of order 4 and cut frequency of 4 Hz to remove the fast oscillations due to background noise, and then converted from Volts to Kilograms rather than to Newtons.

3.2.1.1 Indexes extraction about the force profile

The mechanical output represented by the force profile allows the extraction of some meaningful indexes, such as the time required by subjects to contract and to relax the forearm muscles. These two variables are known as rise time and relaxation time.

Specifically, relaxation time has been, to date, a means of characterization of clinical myotonia [30] [29] since it manifests at the end of the muscle contraction preventing a full relaxation. According to literature [41]:

- **Relaxation time** has been computed as the time taken by the force profile to decline from 90% to 10% of the peak value.
- **Rise time** has been computed as the time taken for the rising edge of the force profile to go from 10% to 90% of the peak value.

To compute rise times and relaxation times, a threshold was set at the 50% of the maximum force value to identify a starting point S in the ascending phase of the force profile for each contraction. Then, all the values between 0.5 seconds and 2.5 seconds after the S point were mediated. An example of the process is provided in figure 3.5. In the end, the 90% and the 10% of this mean value were computed and identified both over the ascending and the descending phase of the force profile for each contraction. Rise time was then computed as the time interval occurring between these two points in the rising edge, while relaxation time was computed between these two points in the falling one. Whenever the algorithm identified wrong time intervals because of particular oscillations of the force profile, the rise times and relaxation times were adjusted manually.

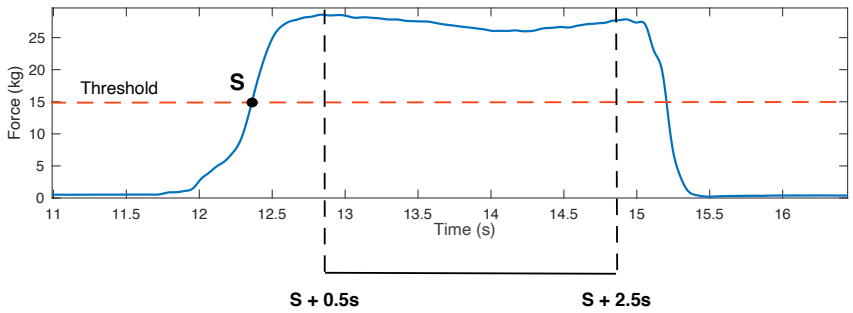

Figure 3.5: Example of the process for the rise and relaxation times computation over the force profile. A threshold was set at the 50% of the maximum force value to identify a starting point (S) for each contraction. A mean value across the points between 0.5 seconds and 2.5 seconds after the S point were mediated. The 90% and the 10% of this mean value were computed.

Figure 3.6 provides an example of the 90% and 10% of the mean across all points in the central portion of each contraction identified in the ascending and descending phase of the force profile.

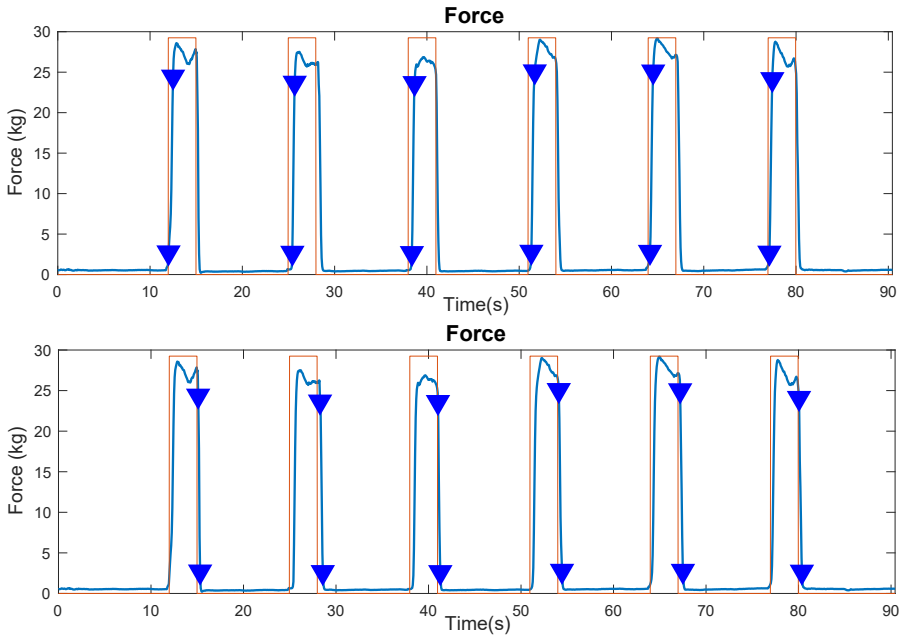

Figure 3.6: 90% and 10% of the mean across the values in the central portion of the each contraction (marked by the blue triangles) identified in the ascending (in the upper portion) and descending (in the lower portion) phases of the force profile in one healthy control (control 3).

Statistical analysis A statistical analysis was performed in order to assess whether rise times and relaxation times were statistically significant different between the group of patients and the one of controls. Two compare the distributions between the two groups, the statistical tests were applied to the subjects' median value across the rise and relaxation times of the six contractions in each set.

To choose the proper statistical test for the comparison, the One-sample Kolmogorov - Smirnov test was performed in order to verify whether the data comes from a standard normal distribution (null hypothesis). Since the test rejected the null hypothesis (meaning that the data under investigation were not normally distributed), the Mann-Whitney U-test was applied to asses the statistical differences

of rise and relaxation times distributions between patients and controls. The Mann-Whitney U-test is a non parametric test that can be used to assess whether two independent samples were selected from populations having the same distribution.

3.2.2 HDsEMG signal processing

3.2.2.1 Signal filtering and alignment

The monopolar HDsEMG signals collected from patients and controls through the electrode grid were processed and analysed off-line. They were bandpass filtered with a Butterworth filter of order 4 with cut frequencies of 20 Hz and 400 Hz. Signal quality was assessed through visual analysis both in the time and frequency domain. In the time domain, bad channels were interpolated with the neighbouring ones. In the frequency domain, the power spectral density was analysed in order to detect whether power line interference was present. When present, power line interference was removed by applying a notch filter (Butterworth stopband filter of order 4) to reject 50 Hz and its harmonics (100 Hz, 150 Hz, 200 Hz, and 250 Hz).

Because of a not perfect synchronism among the three systems during the acquisitions, the signals of the three grids had to be aligned. For the alignment process, a 1-second signal epoch in the initial portion (seconds: 2-3) was taken into consideration from each recorded monopolar signal. The delays between all couples of channels at the grids interfaces was evaluated using the cross-correlation function. Then, the median value of all the delays between the first and the second grid, d_{12}, was computed, as well as, the one between the second and the third grid, d_{23}. Signals were aligned in the frequency domain to overcome the limitations of the sampling in the time domain. The signals recorded from the second matrix were aligned to the first according to the delay d_{12}, while the third matrix was aligned to the first according to the delay $d_{23} + d_{12}$. An example of the signals after the alignment process is shown in figure 3.7. From the superimposition of the signals of rows four-five and eight-nine, it is possible to observe the effect of the alignment process. As a result of the choice to consider the median value of all delays, not every couple of channels was perfectly aligned. Indeed, the real delay between some couples could be slightly different from the median value.

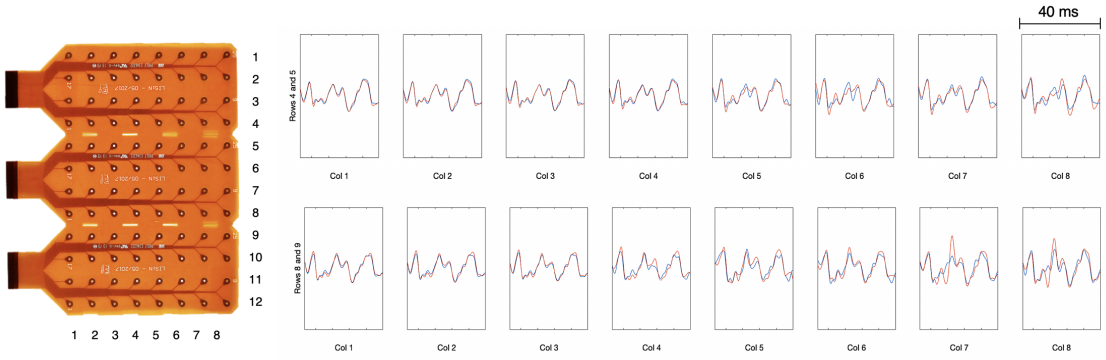

Figure 3.7: Example of the EMG signals recorded from one subject while pressing the little finger against the thumb to show the effect of signal alignment. On the upper portion the superimposition of the signals at the interface between the first (blue) and the second (red) grid, on the lower portion the superimposition of the signals at the interface between the second (blue) and the third (red) grid.

3.2.2.2 Muscle activity detection

In order to analyse the differences in muscles activation and deactivation intervals between patients and controls, muscle on-off timing was estimated. To this purpose, the method proposed by Merlo et al. in [33] was used. This method recognises muscle activity looking for MUAPs in the sEMG recording on the basis of a physical model of muscle activation. Indeed, the sEMG signal can be seen as the sum of MUAP trains and additive noise *n(t)*, analytically described by Eq. 3.1 and 3.2:

$$s(t) = \sum_i MUAPT_j + n(t) \tag{3.1}$$

$$MUAPT_j(t) = \sum_i k_j * f(\frac{t - \theta_{ij}}{\alpha_j}) \tag{3.2}$$

Being j a specific MU, k_j an amplitude factor, θ_{ij} the occurrence times of the MUAPs of the MU, and α_j a scaling factor.

In this scenario, the presence of MUAPs on sEMG recordings can be identified through the Continuous Wavelet Transform (CWT) described by Eq. 3.3.

$$CWT(\alpha, \tau) = (\frac{1}{\sqrt{a}}) \int_{-\infty}^{+\infty} s(t) w^*(\frac{t - \tau}{a}) dt \tag{3.3}$$

Where *w(t)* is the *mother wavelet*, τ is a translation index, and a is a scale parameter (a>0) accounting for the frequency content. The MUAP shape is represented by a specific function that changes on the basis of the detection modality. In details, the zero order Hermite-Rodriguez function (HR_0) may be used in case of monopolar recordings (Eq 3.4), while the first order Hermite-Rodriguez function (HR_1) may be used in case of differential recordings (Eq 3.5) (see figure 3.8).

$$HR_0(t) = -\frac{1}{\sqrt{2\pi}} e^{-(\frac{t}{l})^2}; \tag{3.4}$$

$$HR_1(t) = \frac{2t}{\sqrt{2\pi}} \frac{1}{l^2} e^{-(\frac{t}{l})^2}; \tag{3.5}$$

Where $l = 2^{-n}$ and n is the parameter that has to be changed in order to generate scaled versions of the MUAP. The range for the n parameter was set from N_1=6 to N_2=10, generating MUAPs with temporal support from 15 ms to 5 ms.

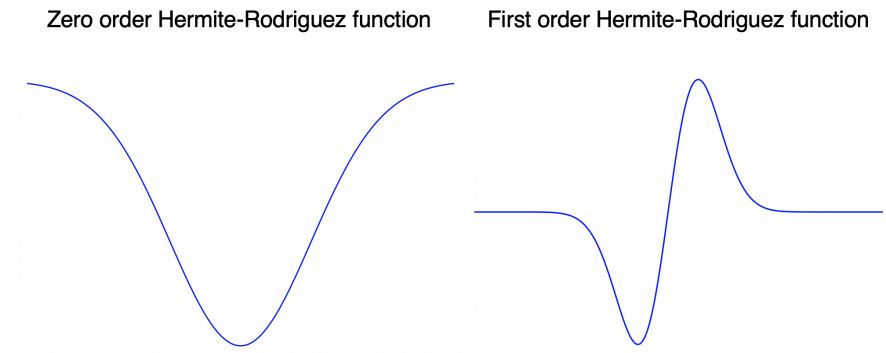

Figure 3.8: On the left, the zero order Hermite-Rodriguez function that match the shape of the potential in monopolar recordings. On the right, the first order Hermite-Rodriguez function that match the shape of the potential in differential recordings.

The event detection is performed by scaling in amplitude and temporal support these functions to match the MUAP shape. Thus, the CWT results in a bank of filters with different degrees of matching between the mother wavelet and the specific

MUAP. The best matched scale is chosen looking for the optimal filters, which are the ones with highest peak in correspondence to the MUAP relative to the peak value without the MUAP. Then, on the basis of the noise level (for $0 < t < T_{noise}$), an amplitude threshold is defined to identify the time periods during which the threshold is overcome (Eq 3.6 and 3.7).

$$M = \max[\max_{a} CWT(a,t)] \tag{3.6}$$

$$th = \gamma * M \tag{3.7}$$

Where γ>1. In the best case, one single set of variables should be able to identify muscle on-off timing for all the subjects under investigation. Nevertheless, the analysis of the recorded signals revealed the presence of background noise with different amplitude from one recording to another and the presence of background noise with different amplitudes in different portions of the same recording. For the previous reasons, it was not possible to identify the same noise threshold, as well as the same time interval in which only noise was present for all the controls and patients. Thus, a visual and specific-case analysis was carried out for each subject. The resulting optimal sets of γ parameter and noise intervals are summarized in table 3.1.

Study partecipants	γ	$T_{NOISE_1}(s)$	$T_{NOISE_2}(s)$
Controls 1, 8, 9	1.2	2	8
Control 2	1.2	18	22
Controls 3, 6, 10	1.2	84	88
Control 7	1.2	5	10
Patients 1, 8	1.2	5	10
Patient 2	1.2	7	10
Patient 4	1.1	5	10
Patient 5	1.2	85	90
Patient 6	1.2	84	88

Table 3.1: Noise-related time interval (where T_{NOISE_1} and T_{NOISE_2} denote respectively the starting and ending point of the time interval) and γ parameter for each subject for the identification of muscle on-off pattern.

After the detection process, a post-processing procedure is applied. A detected spike with duration smaller than 5 ms is rejected because attributed to isolated MUAPs or noise related spikes; two detected activation intervals which are distant less than a time interval corresponding to 150 ms are merged because considered as belonging to the same contraction. The time interval of 150 ms corresponds to a firing rate of 7pps, selected as the minimum firing rate to consider the muscle active. In this way, the algorithm identifies the time intervals corresponding to muscle activation. An example of the final result is provided in figure 3.9, where the detected muscle on-off timing is superimposed to muscle activation.

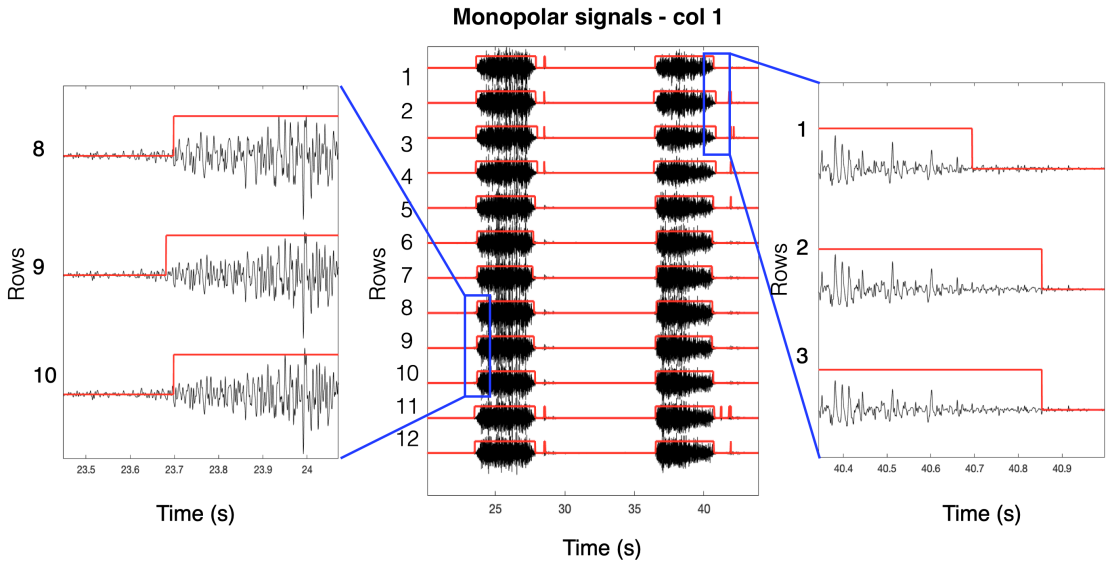

Figure 3.9: In the central portion, muscle on-off intervals (in red) identified during two of the six maximal voluntary isometric grip contractions on control 7 on monopolar signals (in black). The signals recorded by the electrodes in column 3 of the grid are shown. On the right an enlargement of rows 7, 8, and 9 in the last phase of the contraction; on the left an enlargement of rows 5, 6, and 7 in the initial phase of the contraction.

Since the grid was composed by a total of 96 electrodes, in each of them a different pattern of activation may be identified depending on the muscles or muscle portions underlying the electrodes. In order to obtain an overall muscle activation pattern was extracted, the sum of the activation profiles of each channel was computed and

only the segments that overcame a threshold were considered. The threshold was set to the 85% of the total number of channels for the monopolar configuration and 30% of the total number of channels for the Single Differential filter (SD) one. An example of the process for the extraction of an overall muscle activation profile is provided in figure 3.10.

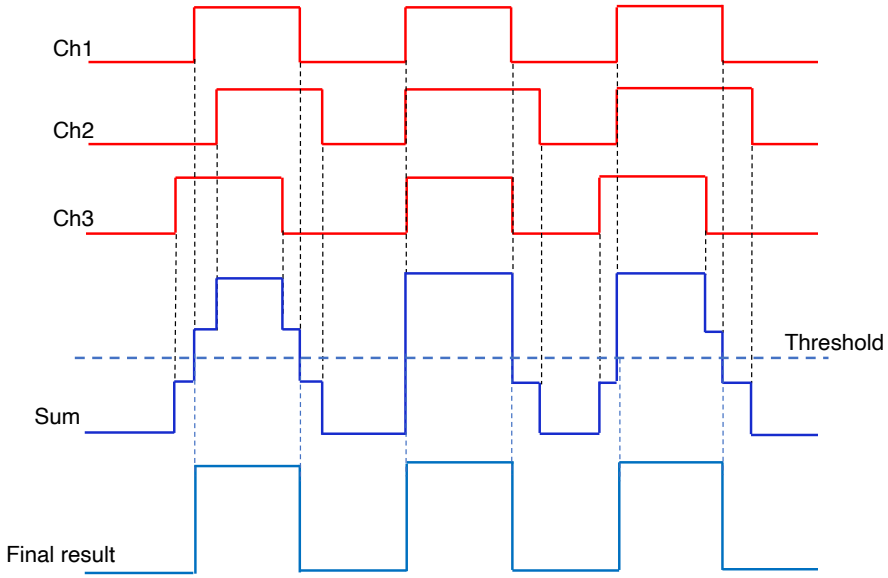

Figure 3.10: Example of the process to obtain the overall muscle activation pattern. At first, the sum of the activation profiles of each channel was computed and a threshold (depending on the type of recording and the total number of channels) was set. Lastly, the overall muscle activation pattern was extracted by all the segments that overcame the threshold.

Global information related to muscle activity were expected to highlight a prolonged overall muscle activity with respect to the declining phase of the force profile in patients. To correlate the time required by muscles to relax with the relaxation phase of the mechanical output, the interval of time occurring between the descending phase of the force profile and the end of the estimated muscle activity was computed for all the six contractions in each set. Specifically, the 90% of the mean across the force values in the 3s-contraction interval was computed and identified over the falling edge of the force profile. Then, the deviation between this point and

the end of the previously computed overall muscle contraction was calculated (see figure 3.11). A high time deviation was considered an index of the difficulty to relax muscles when the myotonic phenomenon occurred.

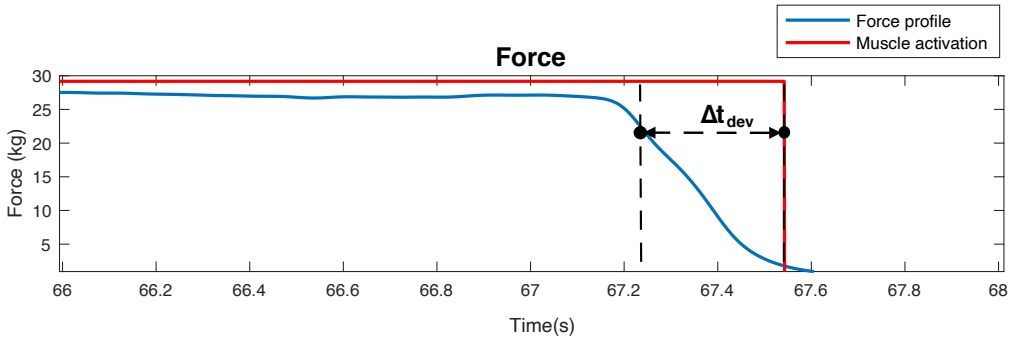

Figure 3.11: Superimposition of the overall muscle activation profile (in red) and the force profile (in blue) during one MVC contraction. To correlate the mechanical output relaxation phase and muscle relaxation phase, the interval of time occurring between the end of muscle activation and the point at the 90% of the mean across the force values during the 3-s contraction was computed.

3.2.2.3 HDsEMG signal decomposition

Muscle electrical activity recorded by a detection system is the sum of action potentials of all the active MUs inside the detection volume [15] [34]. Since the result is a random interference pattern, the recorded signal is very difficult to interpret. This is particularly true in the case of surface electromyography where the volume conductor acts as a filter [35] [34]. In this scenario, the possibility to separate the different MUs contributions becomes essential when investigating MUs recruitment. The procedure to determine the discharge patterns and times from electromyographic signals is referred to as EMG signal decomposition and it consists in the identification of the different Motor Unit Action Potential Trains (MUAPTs) from the raw EMG signal [34] (see figure 3.12). Electromyographic signal decomposition allows the extraction of information related to the Central Nervous System (CNS) to study the motor control, such as how motor units are controlled by the CNS in generating force,

MUs recruitment, MU firing rates, correlation of MU firings, but also more complex investigations, such as the latency between MUs firings and force. Moreover, decomposition allows the investigation of MUAPs shape and morphology linked to pathophysiological information of the muscle fibres [36].

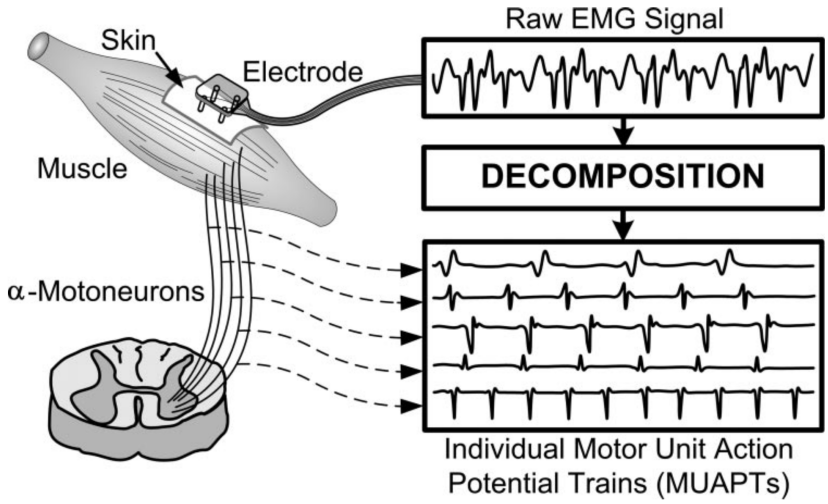

Figure 3.12: Outline of sEMG signal decomposition into its constituent MUAPTs [36]

In vivo, the identification of the action potentials of individual MUs is generally performed by needle EMG for its high spatial selectivity, although representative of only those fibres firing near the recording electrode and not of all the fibres composing the MU [15]. HDsEMG technique is less selective than intramuscular electromyography. Nevertheless, signal decomposition is still possible [37] and several automated signal decomposition techniques have been implemented to decompose surface EMG in its constituent MUAPTs [15] [24] [38] [39] [40]. In these cases, the number of MUs identified is generally smaller than the real number of active MUs because of the high complexity of sEMG signal [39].

With the purpose to investigate central level information, HDsEMG signals from patients and controls were decomposed off-line through the DEMUSE automated signal decomposition tool. DEMUSE tool uses the gradient Convolution Kernel Compensation (gCKC) decomposition technique to identify MUs sequentially. The technique is explained by Holobar et al. in [35] and has been proven suitable both for low

force and high force isometric contractions [37]. The DEMUSE tool identifies MUs in the sEMG recording and estimates MUAPs template by spike triggered averaging of sEMG channels. The detected MUs are then represented by the template of their action potential in terms of shape and location on the electrode grid.

The recorded signals were then loaded into the DEMUSE tool that automatically tested the acquired EMG channels for presence of movement artefacts and bad skin-electrode contacts. The percentage of the EMG channels to be included into the decomposition was set to 95%, meaning that 5% of the channels with the lowest estimated signal quality were discarded. Before running the decomposition process, the time differentiator option was applied to all signals. It is a high-pass filter which suppresses small MUAPs and enhances the discrimination of MUAPs from different MUs for better estimates. The entire signal length was decomposed through 200 iterations and the Common Average Reference (CAR) filter was applied to EMG signals. The application of spatial filter to the signal before starting the decomposition process allows to enhance the shape and occurrence of the different potentials. In particular, the CAR filter subtracts the average of signals across all channels from each channel of the electrode grid. The DEMUSE tool interface and an example of MU template and discharge pattern identified by the tool are shown in figures 3.13 and 3.14.

The accuracy of the decomposition process was assessed by means of the Pulse-to-Noise Ratio (PNR) metric, automatically computed for each identified motor unit according to Eq. 3.8:

$$PNR_i = PNR(t_i(n)) = 10 * \log \frac{E(t_i^2(n)|_{t_i(n)\leq r})}{E(t_i^2(n)|_{t_i(n)<r})} \tag{3.8}$$

being $E(t_i^2(n)|_{t_i(n)\leq r})$ and $E(t_i^2(n)|_{t_i(n)<r})$ the mean across all time instants in which the i^{th} MU is estimated to have or not to have discharged [37]. The PNR metrics is not dependent on regularity of motor unit discharge pattern, thus this parameter is not affected by the irregularity of motor unit discharge patterns caused by pathologies. According to different simulation studies [37], MUs resulting in a PNR $>$ 30 dB show sensitivity in identification of MU discharges $>$ 90% and false alarm rates $<$ 5%. For this reason, all the identified MU with a PNR value lower than 30 dB were discarded.

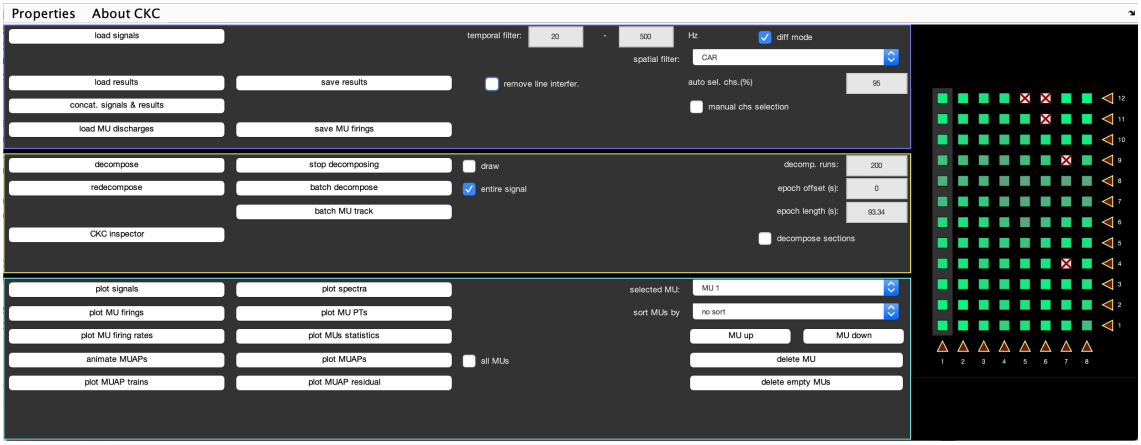

Figure 3.13: DEMUSE tool interface after the loading of signals from a 12x8 electrode grid and parameters setting.

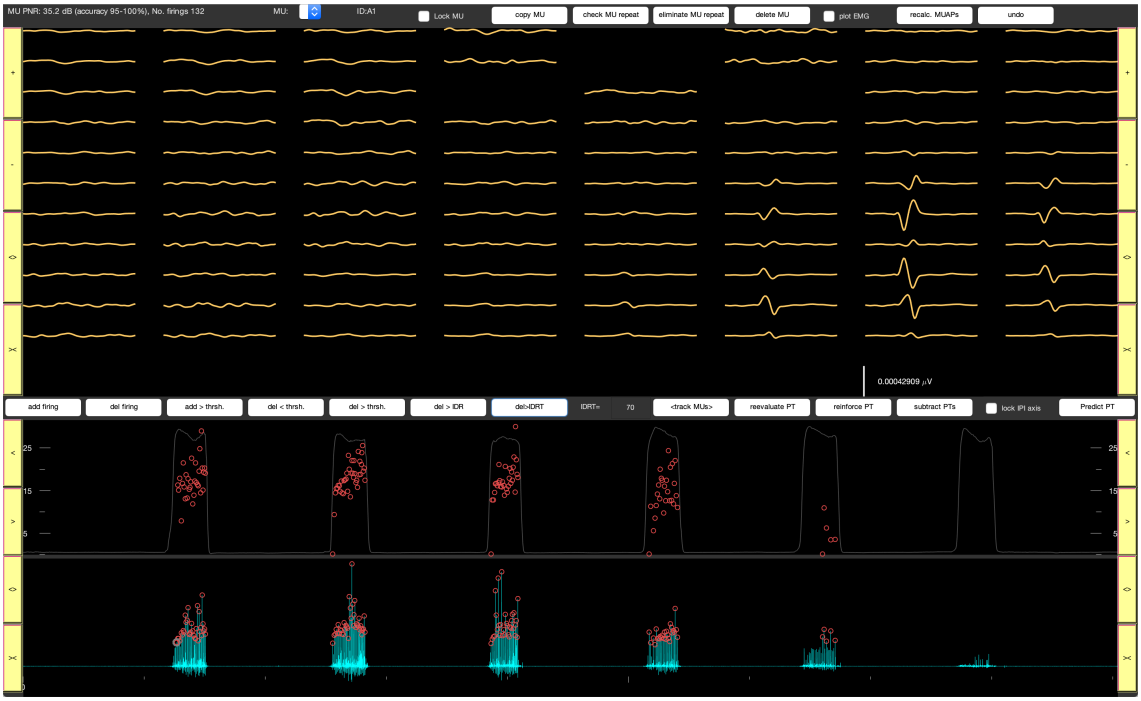

Figure 3.14: Example of MU templates and discharge pattern identified by the DEMUSE decomposition tool. Bad channel are automatically discarded by the tool. In the upper portion the MU template identified through the averaging of EMG signal epochs centred at the MU firing instants. In the lower portion the force profile corresponding to six MVC contractions with the superimposition of the MU instantaneous frequencies and the CKC outcome with the superimposition of the firing instants.

Given the results from DEMUSE tool, discharge patterns and templates should have been visually analysed and manually adjusted. Instead to do so, a posteriori automated analysis was preferred. Thus, MUs templates were automatically estimated from the discharge pattern provided by the DEMUSE tool and the spikes producing instantaneous frequencies higher than 50 Hz (considered a physiological upper limit) were eliminated. Which of the two spikes should have been discarded was chosen according to the output of Convolution Kernel Compensation (CKC) decomposition (in cyan in figure 3.14). In particular, the spike corresponding to the a peak of the filter output with smaller amplitude was discarded, as its occurrence was identified as less probable. MUs templates were estimated by the averaging of signal epochs of 40 ms centred in each of the firing instant for each channel.

Chapter 4

Results

4.1 Introduction

According to the study objectives and the initial hypothesis, HDsEMG and force signals were analysed to investigate the muscles and muscle compartments involved in the myotonic afterdischarge during handgrip, the abnormal motor units' recruitment pattern, the functional impairment, relaxation times and rise times, and levels of muscle strength in patients. Patients' results were compared to controls'.

For the data analysis:

- Two of the eight patients (patient 3 and patient 7) were discarded since they did not have sufficient finger flexor strength to grasp the handle of the dynamometer.
- Two of the ten controls (control 4 and control 5) were discarded for recordings-related problems.

Tables 4.1 and 4.2 provide the patients' information about their pathological condition, force clinical testing revealed by MRC (Medical Research Council) scale, the value of the Muscular Impairment Rating Scale (MIRS), and the Body Mass Index (BMI). The MRC scale refers to the degree of force exerted by the muscles under investigation. The lowest is the number in a range 0-5, the lowest is the level of force exerted. The MIRS scale is specific for MD and is used to classify the degree

of muscular impairment. Specifically, the higher is the number in a 1-5 range, the higher is the muscular impairment. Note that the discarded patients were those with a high level of muscular impairment and, as a consequence, low force levels.

Patients	**Year of birth**	**Sex**	**MD onset**	**Diagnosis**	**Type**	**Therapy**
P1	1991	F	1995	2015	DM1	Yes
P2	1989	M	1999	2015	DM1	Yes
P3	1966	M	1968	2000	DM1	No
P4	1963	F	2000	2014	DM2	No
P5	1979	M	2009	2019	DM1	No
P6	1982	F	1996	1996	DM1	Yes
P7	1962	M	1985	1997	DM1	No
P8	1957	F	-	2000	DM1	No

Table 4.1: Patients' information about their pathological condition.

Patients	**flexors MRC**	**MIRS**	**BMI** ($\frac{kg}{m^2}$)
P1	5	2	22,04
P2	5	2	21,62
P3	3	3	31,49
P4	4	3	22,92
P5	3	3	21,5
P6	5	2	22,66
P7	3	4	24,22
P8	5	2	26,67

Table 4.2: Patients' information about force and muscle clinical testing and body mass index.

While performing the motor task, patients were asked to report whenever they felt the presence of a myotonic discharge. Patients 2, 4, 5 and 6 reported the feeling of myotonia during the first and second of the six contractions in a set. In addition, it was taken into consideration that patient 8 was genetically diagnosed the pathology, but presented no symptomatology.

4.2 Mechanical output analysis

The analysis of the mechanical output provided the possibility to compare patients' and controls' release of grip and grip strength.

4.2.1 MVC contractions

Comparing the patients' force profiles with those of controls, a difference in strength exerted at maximal voluntary contractions was noted. Most patients showed lower levels of muscle strength with respect to controls (except those with 5 in MRC clinical evaluation). In details, forces exerted by controls showed median value of 30,31 kg, 25th percentile of 27,56 kg, and 75th percentile of 37,90 kg; forces exerted by patients showed median value of 18,07 kg, 25th percentile of 10,12 kg, and 75th percentile of 25,88 kg (see figure 4.1). The Mann-Whitney U-test resulted in the identification of a statistically significant difference between the patients' and controls' force distributions with a p-value of 0.02.

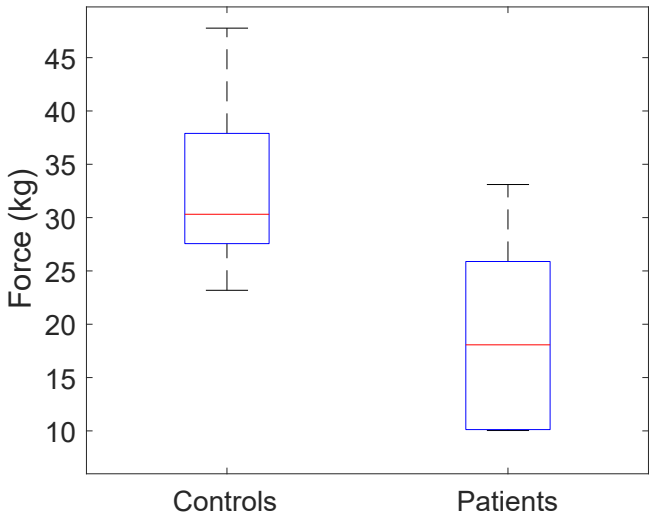

Figure 4.1: Comparison between the ranges of force exerted by controls and by patients during maximal voluntary contractions. To notice the lower levels of forces exerted by patients (median value of 30,31 kg, 25th percentile of 27,56 kg, and 75th percentile of 37,90 kg) than controls (median value of 18,07 kg, 25th percentile of 10,12 kg, and 75th percentile of 25,88 kg).

4.2.2 Indexes about force profile

By the qualitative analysis of the mechanical output profile between patients and controls, a difference at the end of MVC contractions was noted. For the MD group the descending phase of the force profile was characterized by a delayed return to baseline, while in controls, it was almost vertical. In particular, in those patients who reported the feeling of myotonia right after muscle contraction (P2, P4, P5, and P6), a prolonged tail was evident at the end of such contractions. This was evident above all after the first contractions of each set, while the others featured shorten tails. These findings are consistent with the decreasing of symptoms after repetitive contractions, the so-called "warm-up" phenomenon.

The resulting rise times and relaxation times distributions of the eight controls and the six patients for the three sets of contractions are shown in boxplots 4.2 and 4.3. To notice the differences between patients and controls. The latter present the median value of rise times always under 1 second and the median value of relaxation times under 1.5 seconds. In patients, on the other hand, the trend is variable.

The boxplots in figure 4.4 show the group results in terms of median and interquartile ranges. The One-Sample Kolmogorov-Smirnov test rejected the hypothesis of data coming from a standard normal distribution, both for patients and controls. The Mann-Whitney U-test resulted in no statistically significant differences between controls' and patients' rise and relaxation time distributions in none of the three sets of contractions. Nevertheless, a higher trend in patients' distributions with respect to controls can be noted. Table 4.3 contains the p-values from the comparison of rise and relaxation times between patients and controls for each set of contractions.

	p-values		
	SET 1	**SET 2**	**SET 3**
Rise times distributions	0,57	0,75	0,85
Relaxation times distributions	0,14	0,34	0,18

Table 4.3: Mann-Whitney U-test p-values from the comparison of controls' and patients' rise time distributions

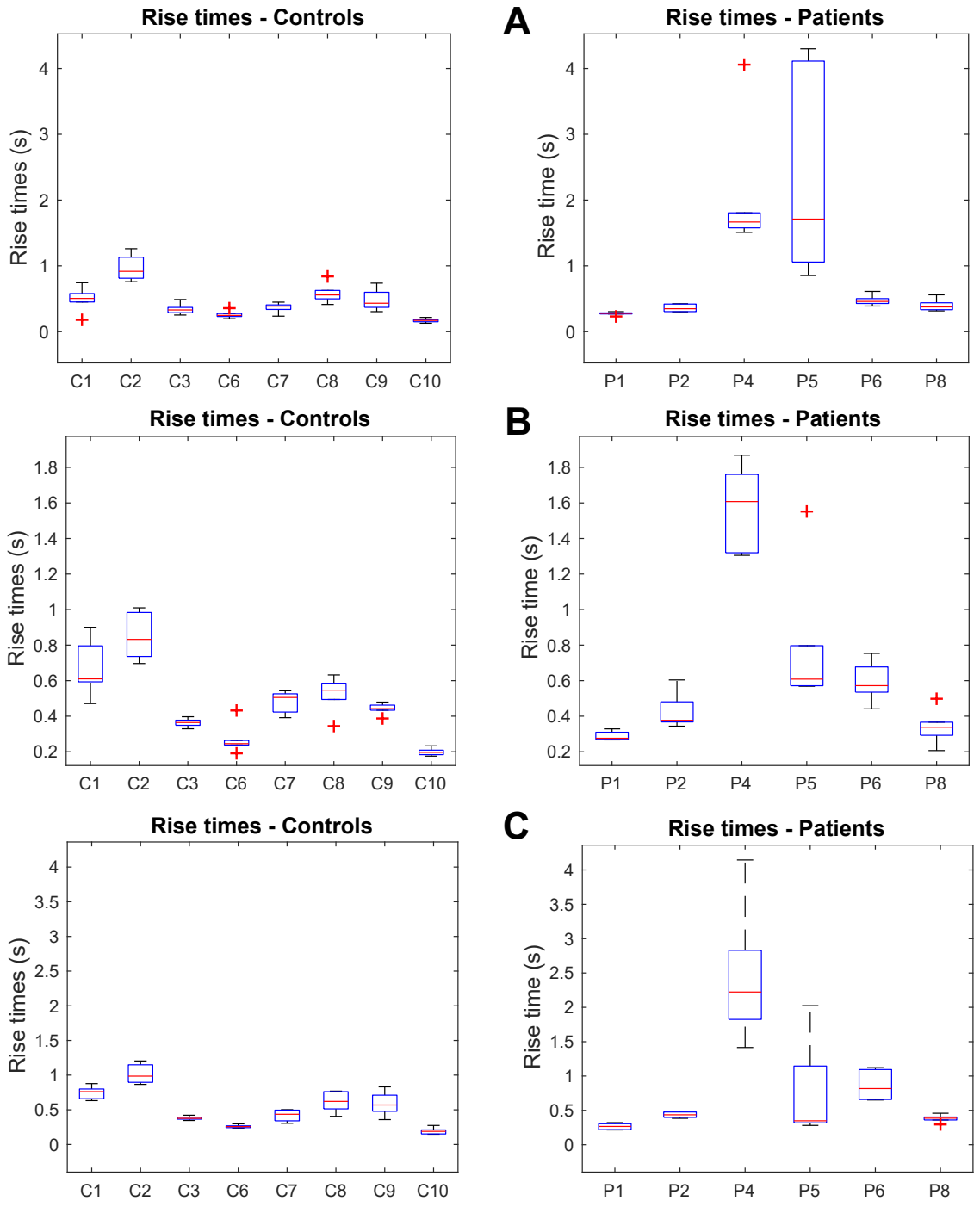

Figure 4.2: Rise times distributions over six contractions for each subject (controls on the left and patients on the right) **A.** Results from the first set; **B.** Results from the second set; **C.** Result from the third set.

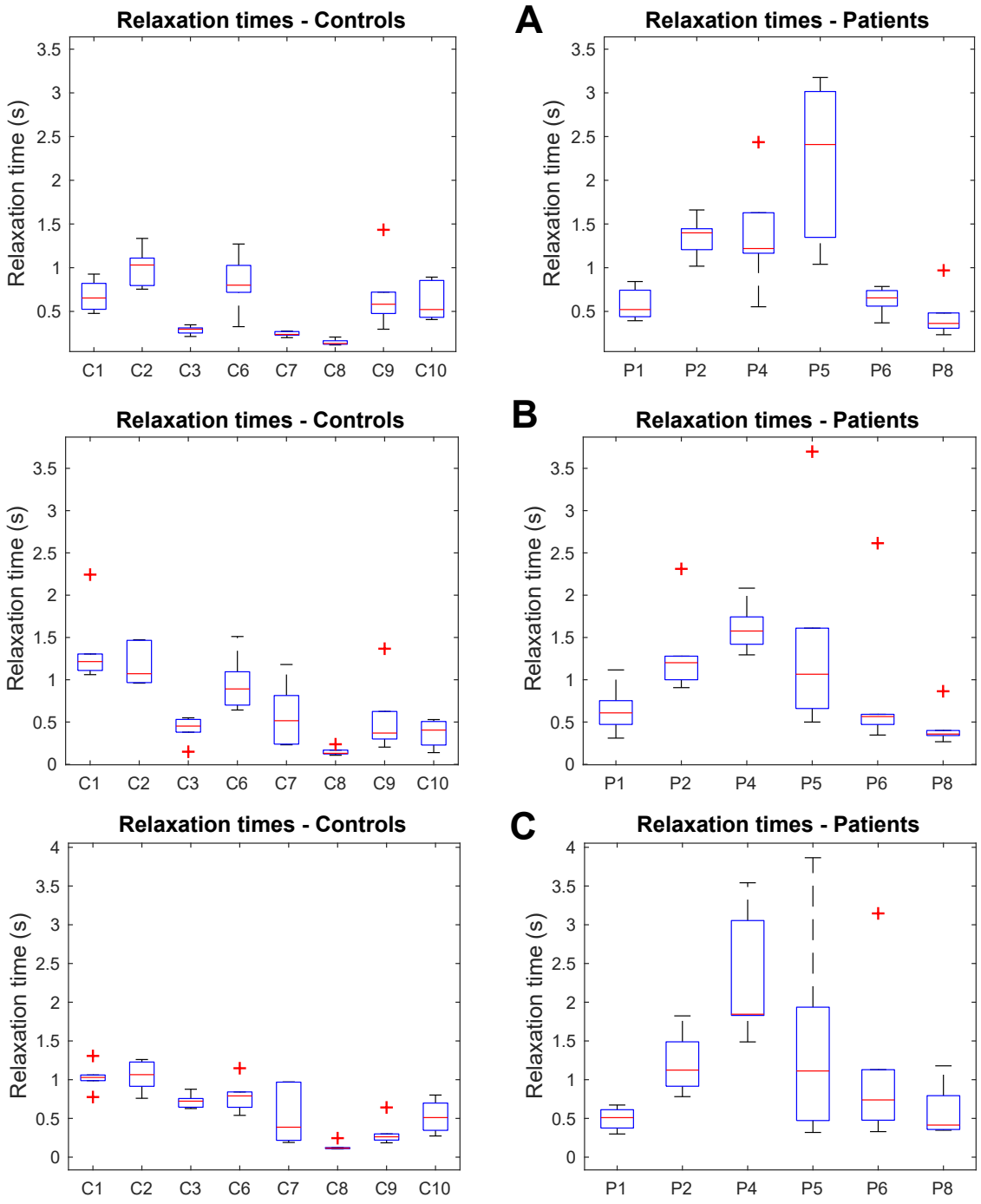

Figure 4.3: Relaxation times distributions over six contractions for each subject (controls on the left and patients on the right) **A.** Results from the first set; **B.** Results from the second set; **C.** Result from the third set.

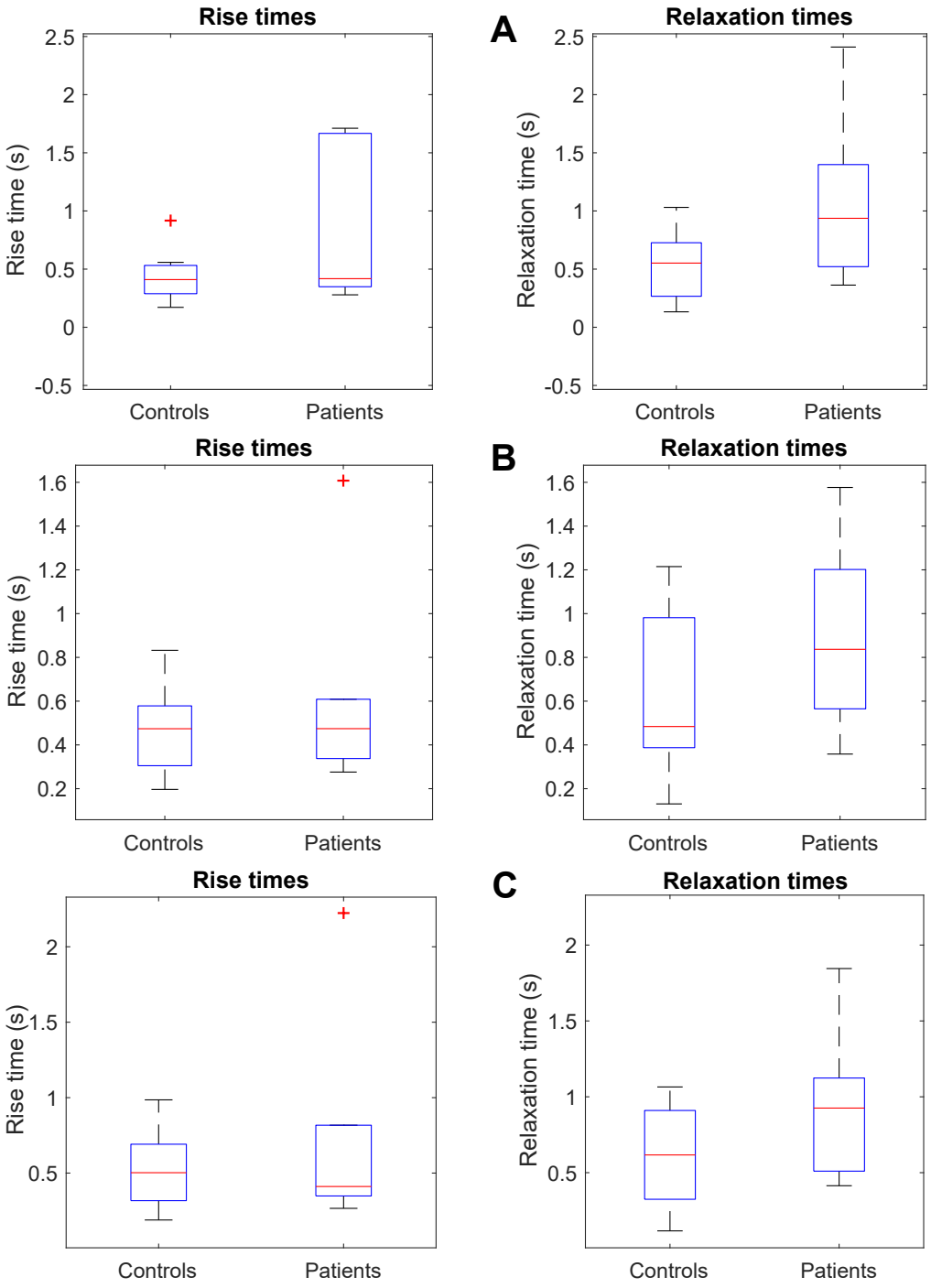

Figure 4.4: Comparison between controls' and patients' rise times (on the left) and relaxation times (on the right). For each subject the median value of six contractions was considered. **A.** Results from the first set; **B.** Results from the second set; **C.** Results from the third set.

4.3 EMG activation analysis

4.3.1 Muscle activity detection

In the control group muscle activation and deactivation pattern behaved the same in every subject following the rising and falling edges of force profile as index of a normal condition. Figure 4.5 provides an example of muscle on-off timing detected in one of the healthy subjects.

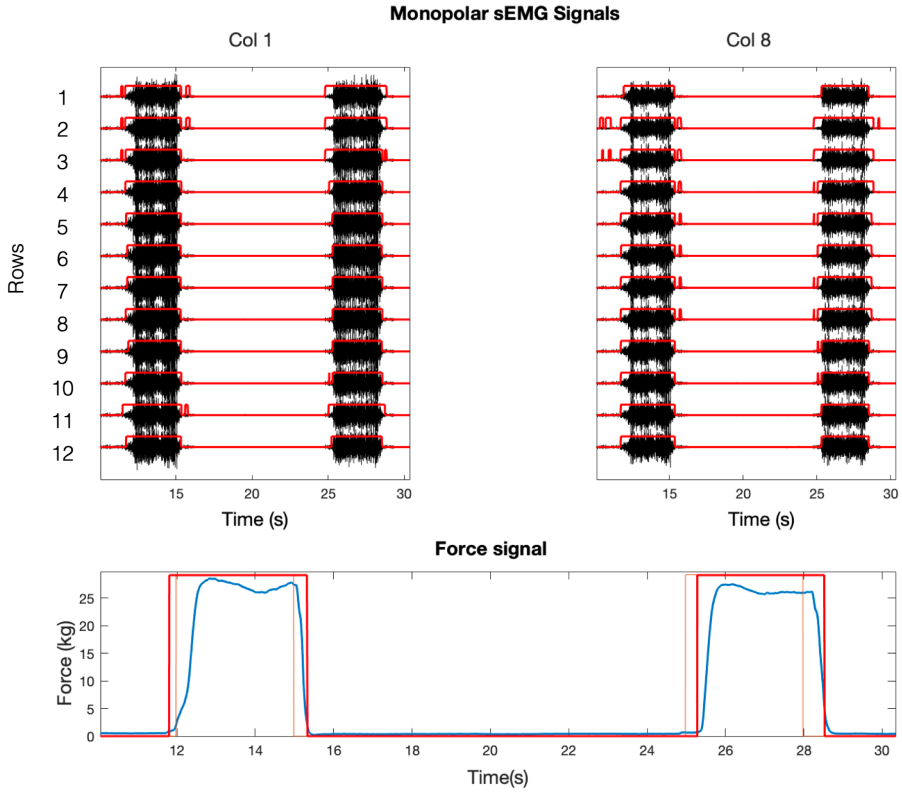

Figure 4.5: The first two of six contractions from a representative healthy subject (control 3). In the upper portion the monopolar signals recorded from the first and the last columns of the electrode grid (in black) with the superimposition of the detected muscle on-off timing (in red). In the lower portion the recorded force signal (in blue) and the ideal trend (in orange) with the superimposition of the overall muscle activity profile (in red). Muscle activation and deactivation is congruent with the rising and falling edges of the force profile.

As for patients, results differed according to the different features of the mechanical output profile and electrophysiological recordings. In particular, in patients P1, P6 and P8 the overall muscle activation and deactivation profile was found to be congruent with the rising and falling edges of the force profile, as in healthy subjects. Interesting results came from the muscle activation and deactivation pattern of P2 and P5. In details, patient 2 muscle on-off pattern resulted in a prolonged muscle activity with respect to the descending phase of the mechanical output, as shown by figure 4.6.

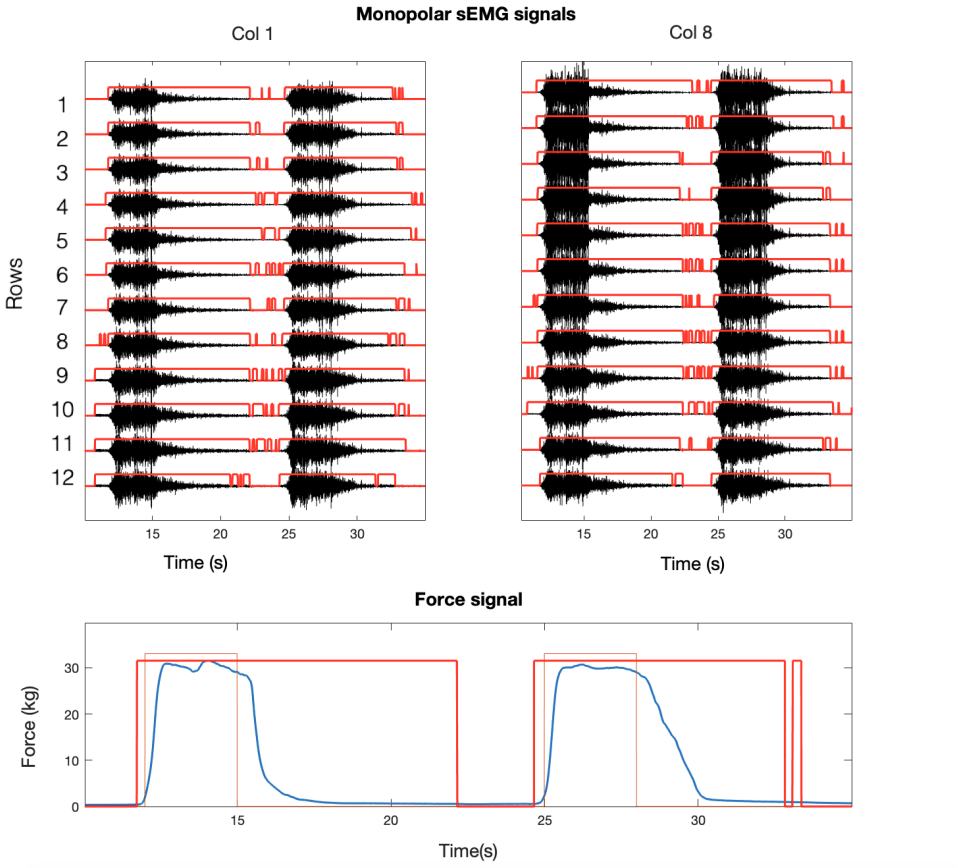

Figure 4.6: The first two of six contractions from patient 2. In the upper portion the monopolar signals recorded from the first and the last columns of the electrode grid (in black) with the superimposition of the detected muscle on-off timing (in red). In the lower portion the force signal (in blue) and the ideal trend (in orange) with the superimposition of the overall muscle activity profile (in red).

Patient 5' sEMG recordings reported the presence of a high and continuous interference pattern. Nevertheless, in this case, the last seconds of the recording reported no muscle activity and were then specified as noise interval. The leftover part of the recording was characterized by an almost continuous muscle activity and, thus, identified as such. Also in patient 5, a prolonged muscle activation with respect to the relaxation phase of the mechanical output was identified, as shown in figure 4.7.

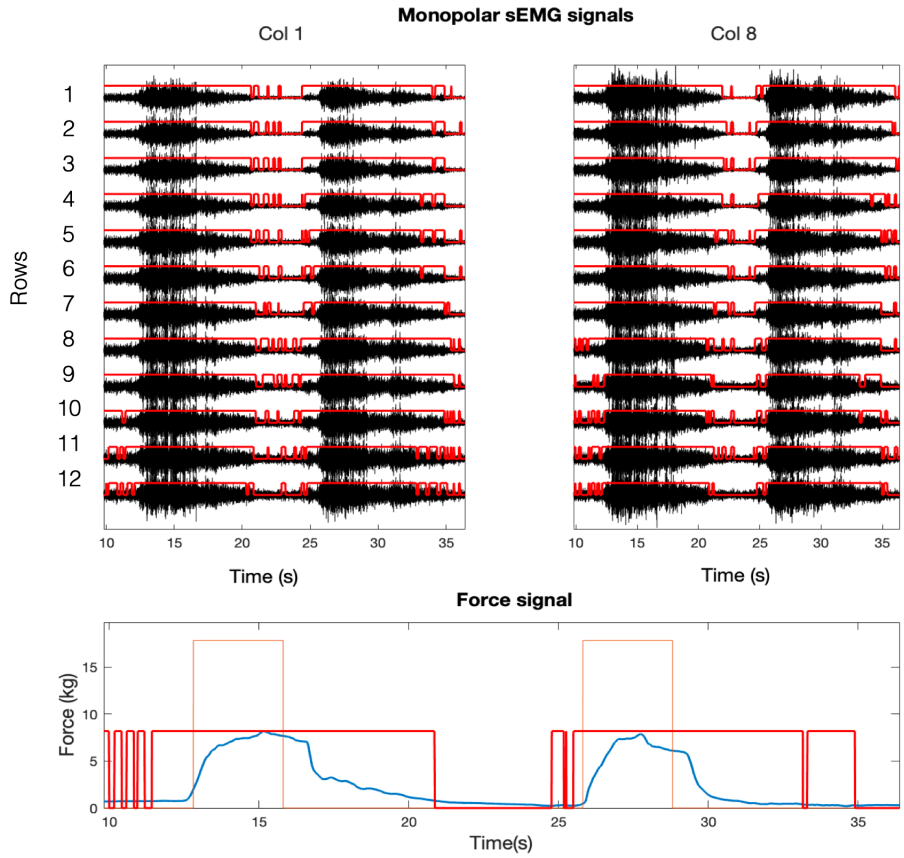

Figure 4.7: The first two of six contractions from patient 5. To notice the difficulty in release the grip. In the upper portion the monopolar signals recorded from the first and the last columns of the electrode grid (in black) with the superimposition of the detected muscle on-off timing (in red). In the lower portion the force signal (in blue) and the ideal trend (in orange) with the superimposition of the overall muscle activity profile (in red).

Critical issues were encountered in the muscle activity detection of P4 in which sEMG recordings were characterized by a higher interference pattern than controls even during the relaxation phases. Being the performances of the method dependent on the presence of time intervals in which no muscle activity is present, muscle activation was underestimated. Indeed, in this case, while decreasing, muscle activity became comparable to the background interference pattern indicated as noise threshold and, thus, not identified (see figure 4.8).

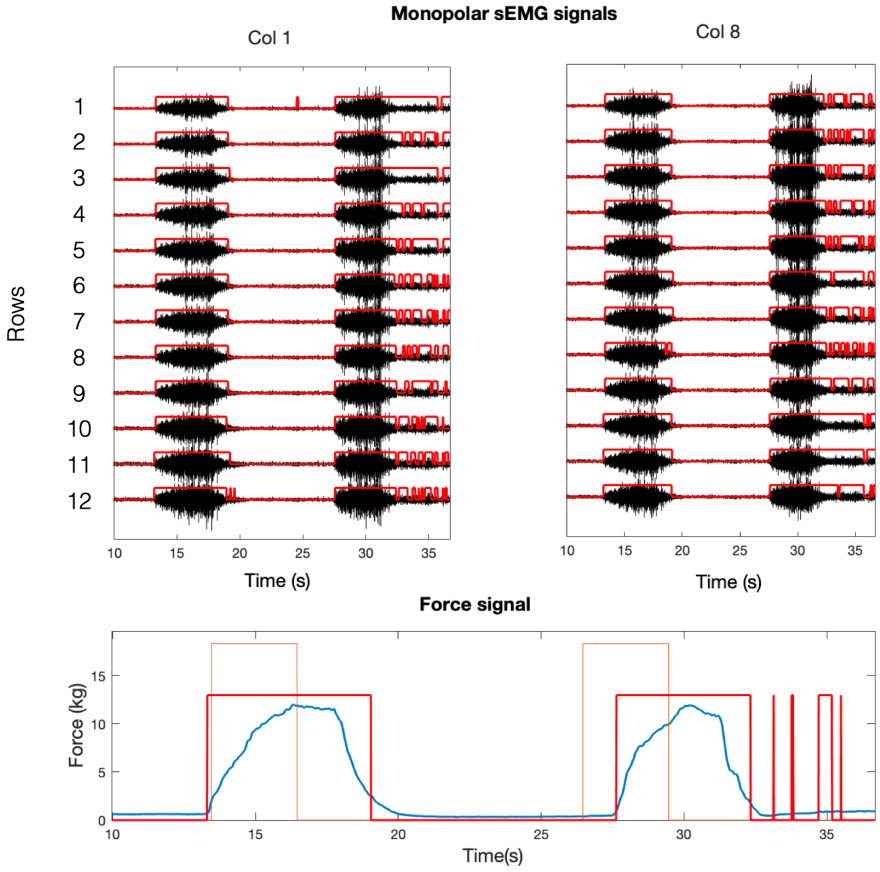

Figure 4.8: The first two of six contractions from patient 4. To notice the underestimation of muscle activity in the falling edge of the force profile after the first contraction and at the beginning of the recording. In the upper portion the monopolar signals recorded from the first and the last columns of the electrode grid (in black) with the superimposition of the detected muscle on-off timing (in red). In the lower portion the force signal (in blue) and the ideal trend (in orange) with the superimposition of the overall muscle activity profile (in red).

4.3.2 Correlation between muscle deactivation and force relaxation curve

The scatter plot of figure 4.9 displays the correlation between the time required for muscle relaxation and the relaxation time interval evaluated from the mechanical output. Being the myotonic afterdischarge more evident in the first contractions and getting better with repetitive contractions, only the first set was analysed. The correlation was assessed through the Spearman's test returning a correlation coefficient rho equal to 0.8141, meaning that the two variables are highly correlated. Therefore, it is possible to assert that when the time required to muscles to achieve a fully relaxation status increases, the grip is slowly released as a consequence, thus bringing to a higher relaxation time identified over the mechanical output.

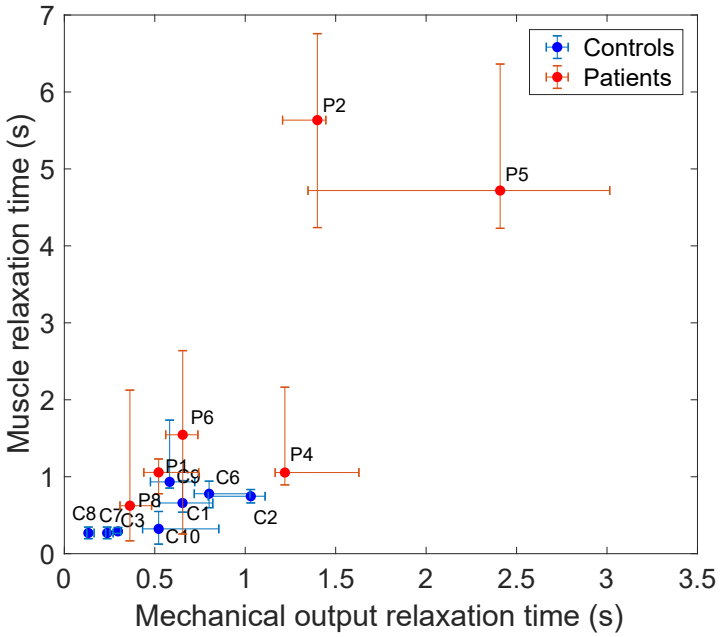

Figure 4.9: Scatter plot of the time required to muscles to relax with respect to the relaxation time identified by the mechanical output. Results refer to the first set of contractions. The median of all controls' (in blue) and patients' (in red) of muscle relaxation times across the six contractions and the respective interquartile ranges (25th and 75th percentiles) are shown.

By the observation of the scatter plot, the split of subjects into two clusters can

be noted:

- one cluster characterized by short mechanical and muscle relaxation times (both under 1.5 seconds) including all healthy subjects and patients 1, 4, 6 and 8;
- one cluster characterized by high mechanical and muscle relaxation times (from 4.5 s to 5.6 s for muscle relaxation and from 1.4 s to 2.5 s for mechanical output relaxation) including patients 2 and 5.

4.3.3 HDsEMG signal decomposition

The automated signal decomposition tool, DEMUSE, identified the presence of MUs firing with a physiological recruitment pattern in controls, which were recruited at the beginning of muscle contraction with increasing firing rates while the force exerted increased, and de-recruited while releasing the grip with a decrease in firing rates, (as shown in figure 4.10).

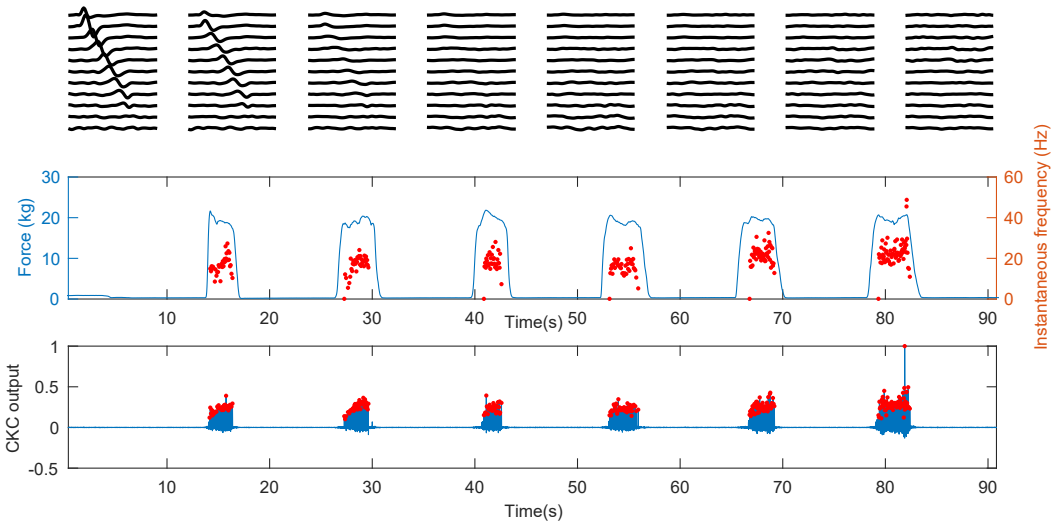

Figure 4.10: Example of a motor unit identified in one healthy subject (control 1) that show physiological recruitment pattern and firing rate. In the upper portion the MU template; in the middle portion the instantaneous frequencies (red spots) superimposed to the force profile; in the lower portion the outcome of CKC algorithm (in blue) with the superimposition of MU discharges (red spots).

However, the majority of MUs identified by DEMUSE tool in both controls and pathological subjects showed high instantaneous firing frequencies and irregular firing pattern (see figure 4.11). This could be due to the merging of more than one MU in a single one. For this reason, the results from the decomposition process were revised manually. Anyway, it was not possible to overcome this limitation of the decomposition tool correlated with high contraction levels that imply a high number of recruited MUs.

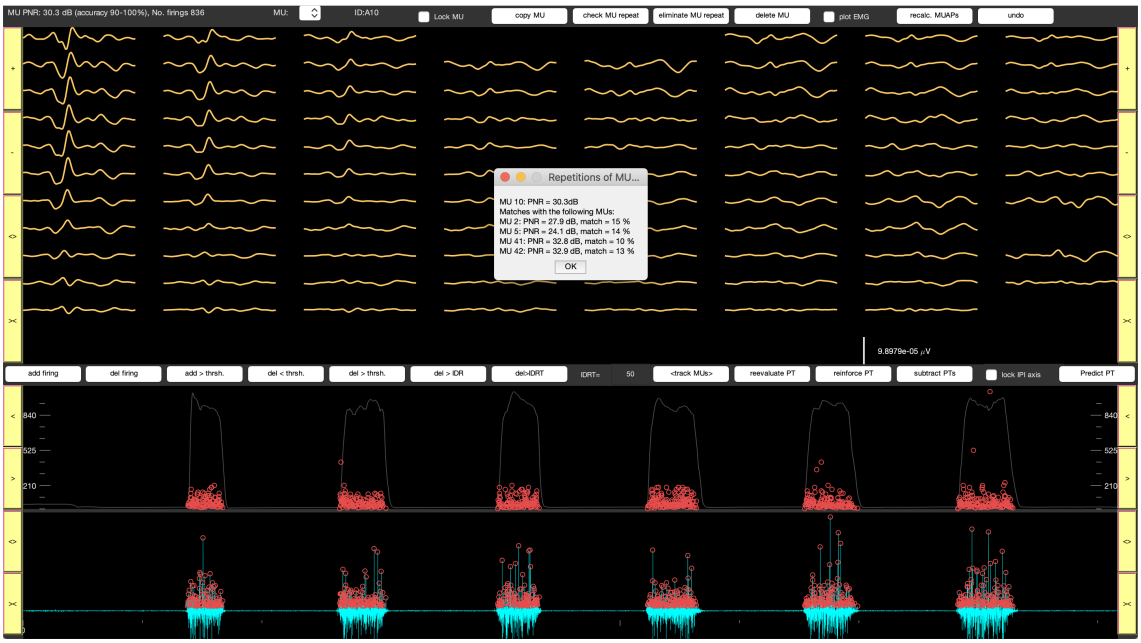

Figure 4.11: Example of a motor unit identified in one healthy subject (control 1) that showed a very high firing rate probably for the merging of more than one MU in a single one.The check for the repetition of the identified MU shows the percentages of match with other MUs. In the upper portion the MU template; in the middle portion the instantaneous frequencies (red spots) superimposed to the force profile; in the lower portion the outcome of CKC algorithm (in blue) with the superimposition of MU discharges (red spots).

As for patients, P1, P6 and P8 showed the same recruitment and de-recruitment pattern identified in healthy subjects. Interesting results were obtained in P2 and P5, where the decomposition tool identified the presence of few MUs firing during the relaxation phase of the force profile. Figures 4.12 provides an example of one

of these MUs. Figures 4.13 and 4.14 present examples of the MUs showing abnormal activity for patient 2 and for patient 5. In patient 4 very few MUs with the aforementioned abnormal recruitment pattern were identified by the decomposition tool. This abnormal condition was present in none of the healthy subjects. These findings are consistent with the results presented in sections 4.3.1 and 4.3.2 by the identification of muscle on-off timing and the correlation of muscle relaxation with the mechanical output profile.

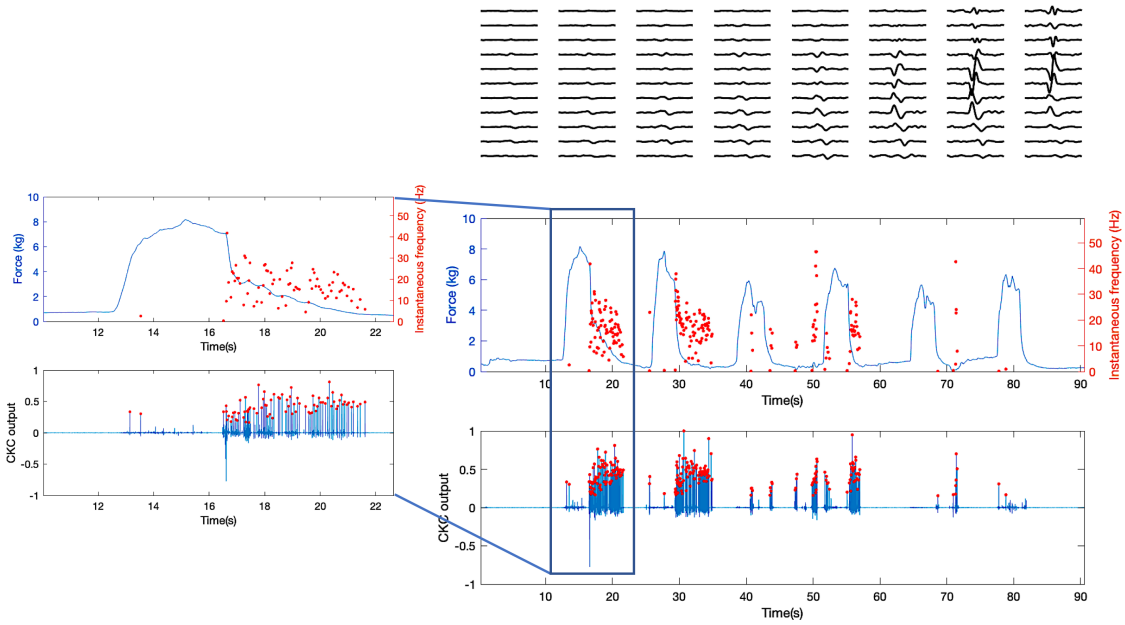

Figure 4.12: Example of MUs firing during the relaxation phase of the force profile identified by the DEMUSE tool. On the right the MUAP template (on the top) and the firing pattern (red spots). On the left, a zoom over the first contraction.

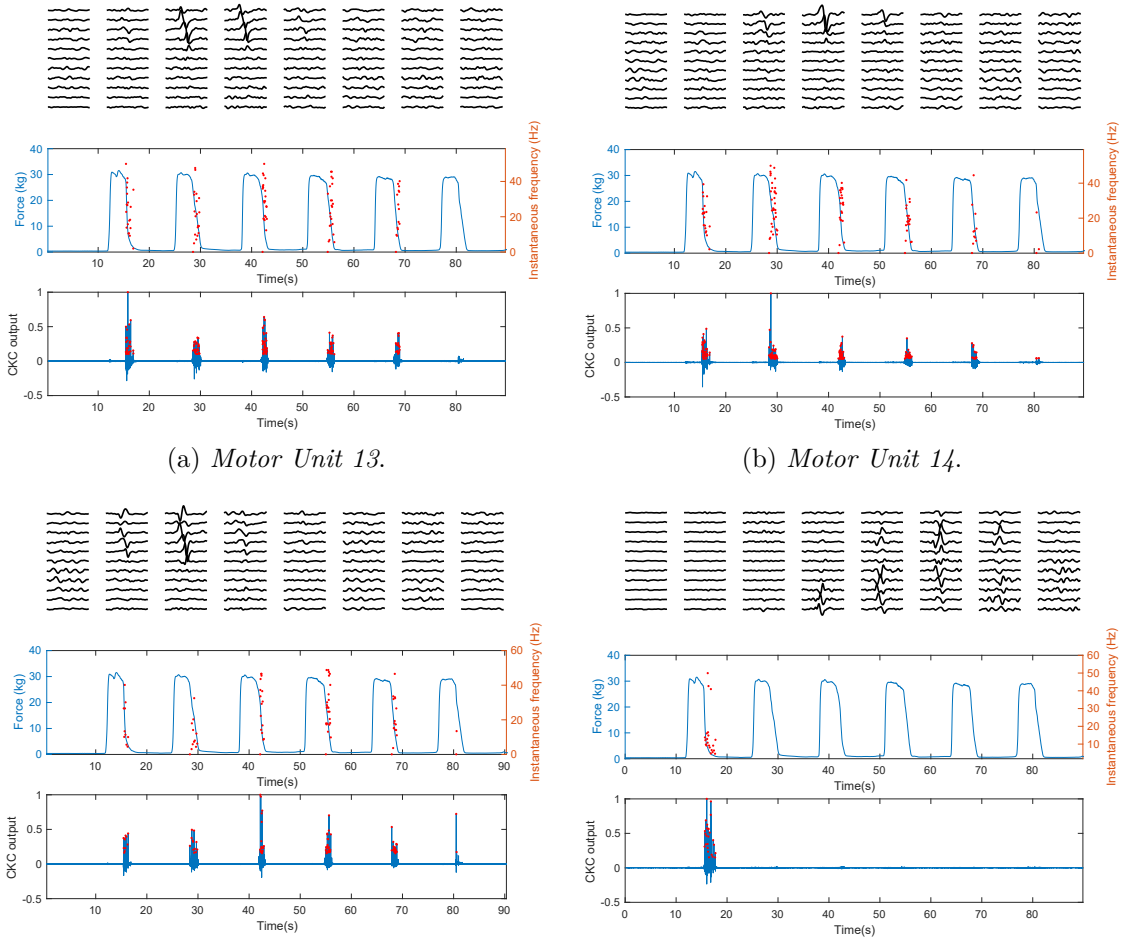

(a) *Motor Unit 13.*

(b) *Motor Unit 14.*

(c) *Motor Unit 19.*

(d) *Motor Unit 26.*

Figure 4.13: Example of MUs identified during the relaxation phase of muscle contraction in patient 2. For each MU, in the upper portion the MU template; in the middle portion the instantaneous frequencies (red spots) superimposed to the force profile; in the lower portion the outcome of CKC algorithm (in blue) with the superimposition of MU discharges (red spots).

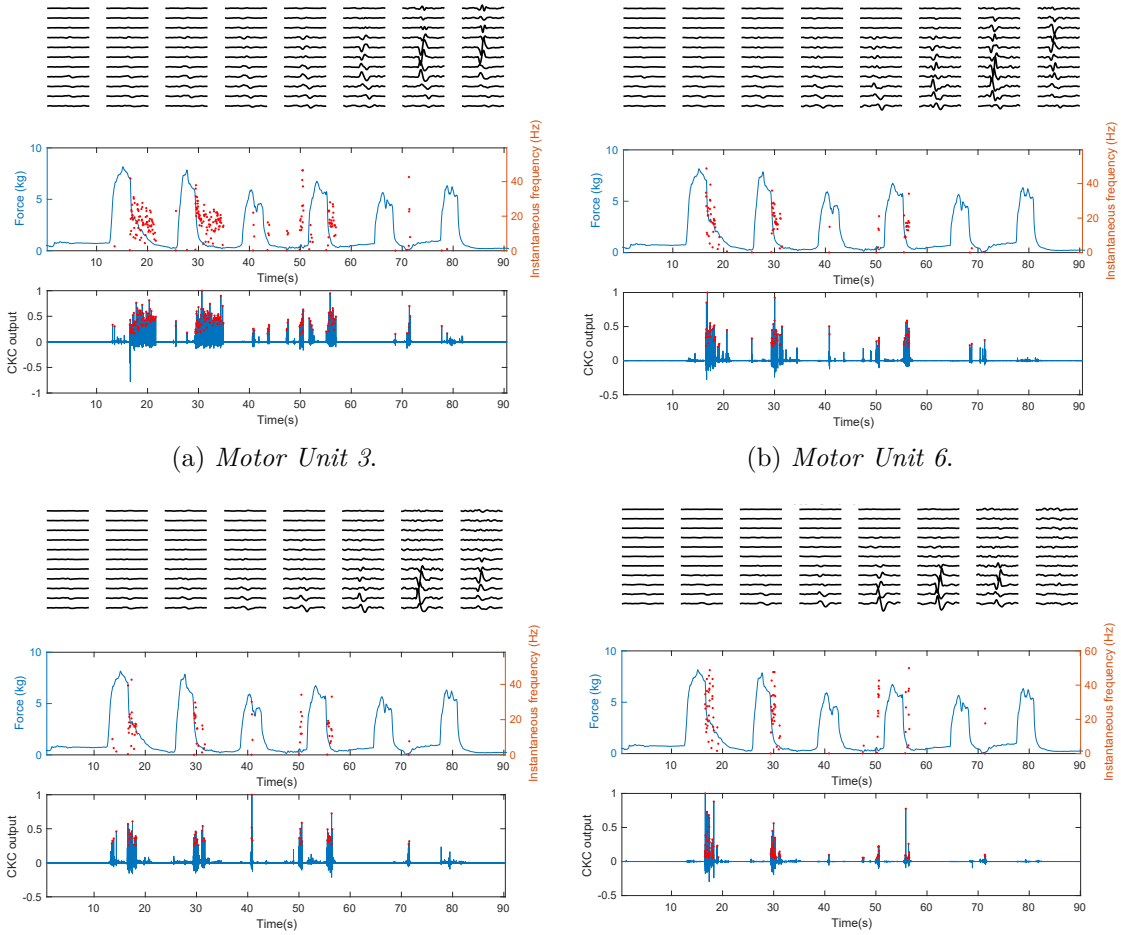

(a) *Motor Unit 3.*

(b) *Motor Unit 6.*

(c) *Motor Unit 8.*

(d) *Motor Unit 13.*

Figure 4.14: Example of MUs identified during the relaxation phase of muscle contraction in patient 5. For each MU, in the upper portion the MU template; in the middle portion the instantaneous frequencies (red spots) superimposed to the force profile; in the lower portion the outcome of CKC algorithm (in blue) with the superimposition of MU discharges (red spots).

Chapter 5

Discussions and conclusions

5.1 Introduction

The present study aimed at investigating grip myotonia in MD through non-invasive measurements of the electrophysiological activity by means of multiple closely spaced surface electrodes (the so-called High-Density surface EMG technique) and force recordings. The use of grids of electrodes allowed to sample the muscular activity over the most of the ventral forearm area of patients and healthy subjects in order to properly investigate flexors muscles activation in the forearm. The recorded sEMG and force signals were processed to identify indexes related to the force profile, to detect muscle activation and deactivation, and to decompose the sEMG signal into the contributions of its constituent MUs.

5.2 Considerations on muscle activity detection

In the healthy subjects the overall muscle activation and deactivation profile was found to be congruent with the rising and falling edges of the force profile, as expected. Results related to patients varied according to the features of the electrophysiological recordings. In particular, from qualitative analysis, it was noted that sEMG recordings of patients not taking anti-myotonic drugs (P4 and P5) were characterized by a high interference pattern with many units firing at the same time, even during the relaxation phases. This condition was associated to a persistent

contraction status of forearm muscles while the hand was grasping the handle of the dynamometer (particularly true for patient 4 and patient 5). Thus, in patient 4 the detection algorithm resulted in the underestimation of muscle on-off pattern. On the other hand, patients taking anti-myotonic drugs had a more similar muscle activity to controls when totally relaxed leading to a more accurate identification of muscle pattern. The same considerations are true for patient 8, being the one in which the pathology was asymptomatic.

As for muscle on-off timing, a prolonged muscle activation was observed both from the mechanical output and sEMG signal in P2 and P5. The hypothesis that this outcome was the result of the myotonic discharge, was confirmed by the patients' feeling of a sustained muscle involuntary contraction, mainly after the first two contractions. Comparing the condition of perceived myotonia after the first muscle contraction between the two patients (see figures 4.6 and 4.7), it was possible to notice that patient 5 showed more difficulties in releasing the grip, probably suggesting a higher intensity of the myotonic afterdischarge with respect to patient 2 (in which muscles seemed to approach gradually the relaxation condition but with less difficulty).

5.3 Considerations on HDsEMG signal decomposition

While muscle activation and deactivation provided information about the global muscle behaviour, sEMG signal decomposition provided insights into the action of CNS during motor control in pathological conditions. The automated signal decomposition tool, DEMUSE, identified the presence of MUs firing in the latest phases of muscle contraction in patients. These MUs were not identified during the central portion of the contraction, probably because of the high interference pattern during MVC contractions. Under the assumptions that these MUs were firing even during the maximal voluntary contraction but were not identified by the tool, results suggest a delayed de-recruitment of some motor units that kept firing at the end of muscle contraction, preventing a quick muscle relaxation. The difficulty in release the grip, suggested by the long tail of the force curve, may confirm these hypothesis.

On the contrary, controls displayed signs of a physiological recruitment pattern, in which MUs were recruited at the beginning of muscle contraction and de-recruited while releasing the grip.

Looking further into the disclosed abnormal muscle activity, interesting observations can be made about the location of the MUs templates on the electrode grid. Looking for the correspondence between MUAPs grid location and the underlying muscles, it was possible to hypothesise the muscles taking part to the clinically evident poor muscle relaxation. From the analysis of the MUAPs location in patient 2, MUs territories show to be mainly concentrated in the central part of the electrode grid standing above, approximately, the Flexor Carpi Radialis muscle. In patient 5, MUAPs are mainly distributed in the medial portion, standing above approximately, the Flexor Digitorum Superficialis muscle. However, further investigations should be carried on to validate these assumptions.

5.4 Mechanical output and muscle activity correlation

The analysis of the mechanical output showed the lower ranges of forces exerted by patients than controls, resulting in a statistically significant difference demonstrated by the Mann-Whitney U-test. On the contrary, the statistical analysis related to controls' and patients' rise and relaxation times distributions showed no significant differences between the two groups. Patients' rise times were actually very similar to controls', even though a slight difference could be noted in relaxation times distributions. The rejection of a statistical significant difference between the two groups may be explained by the results shown in the scatter plot of figure 4.9, where the correlation between the time required by the muscles to relax and that identified over the force profile is shown. Observing the scatter plot, the clustering of subjects into two groups could be noted:

- one cluster characterized by short mechanical and muscle relaxation times including all healthy subjects and patients 1, 4, 6 and 8;

- one cluster characterized by high mechanical and muscle relaxation times including patients 2 and 5.

Thus, the results from the statical tests are justified by the fact that four pathological subjects (P1, P4, P6, and P8) belong to the cluster of controls. Only P2 and P5 showed higher relaxation times (both from muscle and mechanical output).

Exploring further the correlation between mechanical and muscle relaxation, results explanations may be found in the observation of HDsEMG and force signals, in conjunction with the level of muscle impairment reported by patients and clinical data. The following considerations may be taken into account:

- Patients 1 and 8 were the patients that most behaved as healthy subjects. Indeed, patient 1 did not perceive any difficulty in relaxing muscles after grip and to perform the requested task. Furthermore, patient 1 was under the effect of anti-myotonic drugs. Patient 8 was genetically diagnosed the pathology but presented no symptoms. Note that these two patients were evaluated as reporting minimal muscle impairment and as able to exert high level of forces according to the MRC and MIRS clinical examinations.

- Patients 6 and 4 were among the four patients that reported the feeling of myotonia during the first contractions. Indeed, patient 6's median value of muscle relaxation is slightly higher than the one referred to the mechanical output. Patient 4, on the other hand, was clinically evaluated with the number 3 in the MIRS scale, meaning a condition of distal weakness. The classification of this patient in the first cluster may be the result of a not accurate identification of sEMG activation and deactivation timing, as explained in section 4.3.1. Because of the presence of a high interference pattern in muscle activity and the impossibility to determine a proper threshold to distinguish it from noise, muscle on-off timing was underestimated.

- Patient 2 and patient 5 are the two patients belonging to the second cluster. They were among the four patients that reported the presence of the myotonic afterdischarge right after muscle contraction. In particular, both patients reported the difficulty to relax muscles mainly after the end of the first and second contractions. In patient 5 muscle activity was detected also during the

relaxation phases. In particular, patient 5 showed extensive difficulties in performing the requested task, thus resulting in substantial relaxation times, both in muscle activity and mechanical output analyses. These findings are consistent with the clinical examinations, being patient 5 among the ones with the highest degree of muscular impairment and lowest grip strength.

5.5 Limitations of the study

This work is a preliminary phase of an extended study that is planned together with Casa di Cura Privata del policlinico. For this reason, the analysed sample of patients is limited. For this reasons, and the wide differences in clinical conditions, it is not possible to reach general conclusions. Therefore, the evaluations should be expanded to a sizeable sample of patients in order to obtain results that might be considered representative of an entire population. Moreover, the analysis of MVC levels of muscle activation brought to the impossibility to decompose the signals reliably during contractions. Then, it is possible to think to a reduction of the contraction level in the continuation of the study.

5.6 Conclusions

The rare and complex pathology of myotonic dystrophy is mainly characterized, among a wide number of symptoms, by the presence of repetitive muscle fibre potential discharges caused by an increased excitability of the muscle membrane. This symptom, known as myotonia, brings to the visible clinical effect of a delayed relaxation of skeletal muscles resulting in muscle stiffness and pain. Needle electromyographic examination represents to date the gold standard for the recording of this abnormal electrophysiological activity. Nevertheless, due to its invasiveness, this technique presents several limitations.

The present study aimed at outline a non-invasive experimental setup to investigate myotonic discharges in patients with MD. With particular reference to the study goals, the quantitative evaluations coming from HDsEMG and from the mechanical output highlighted differences between the groups of patients and healthy

subjects. The investigation of MUs properties through HDsEMG signal decomposition seemed to allow the evaluation of the involvement of specific muscles or muscle regions of the upper limb through the localization of the MUAP templates. In particular, in this case study, signal decomposition appeared to suggest the presence of a delayed MUs de-recruitment during the myotonic discharge that was hypothesised as the cause of the clinical evidence (poor relaxation).

In conclusion, the results obtained in this very beginning phase of the study suggest the necessity to expand the evaluations to a sizeable sample of subjects in order to verify and confirm the potentialities of the proposed technique for the investigation of myotonia.

Bibliography

[1] A. Aldehag, H. Jonsson, J. Lindblad, A. Kottorp, T. Ansved, and M. Kierkegaard, "Effects of hand-training in persons with myotonic dystrophy type 1-a randomised controlled cross-over pilot study", *Disability and Rehabilitation*, vol. 35, no. 21, pp. 1798–1807, 2013.

[2] L. Machuca-Tzili, D. Brook, and D. Hilton-Jones, "Clinical and molecular aspects of the myotonic dystrophies: A review", *Muscle and Nerve*, vol. 35, no. 21, pp. 1798–1807, 2005.

[3] G. Meola and R. Cardani, "Myotonic dystrophies: An update on clinical aspects, genetic, pathology, and molecular pathomechanisms", *Biochimica et Biophysica Acta - Molecular Basis of Disease*, pp. 594–606, 2015.

[4] G. Meola, "Clinical aspects, molecular pathomechanisms and management of myotonic dystrophies", *Acta Myologica*, vol. 32, no. 3, pp. 154–165, 2013.

[5] G. Ho, "Congenital and childhood myotonic dystrophy: Current aspects of disease and future directions", *World Journal of Clinical Pediatrics*, vol. 4, no. 4, pp. 66–80, 2015.

[6] M. K. Hehir and E. L. Logigian, "Electrodiagnosis of Myotonic Disorders", *Physical Medicine and Rehabilitation Clinics of North America*, vol. 24, no. 1, pp. 209–220, 2013.

[7] E. L. Logician, E. Ciafaloni, L. C. Quinn, N. Dilek, S. Pandya, R. T. Moxley, and C. A. Thornton, "Severity, type, and distribution of myotonic discharges are different in type 1 and type 2 myotonic dystrophy", *Muscle and Nerve*, vol. 35, no. 4, pp. 479–485, 2007.

[8] M. Douniol, A. Jacquette, D. Cohen, N. Bodeau, L. Rachidi, N. Angeard, J. M. Cuisset, L. Vallée, B. Eymard, M. Plaza, D. Héron, and J. M. Guilé, "Psychiatric and cognitive phenotype of childhood myotonic dystrophy type 1", *Developmental Medicine and Child Neurology*, vol. 54, no. 10, pp. 905–911, 2012.

[9] T. Kurihara, "New classification and treatment for myotonic disorders", *Internal Medicine*, vol. 44, no. 10, pp. 1027–1032, 2005.

[10] V. Sansone, K. Marinou, J. Salvucci, and G. Meola, "Quantitative myotonia assessment: An experimental protocol", *Neurological Sciences*, vol. 21, pp. 971–974, 2000.

[11] D. Dumitru, *Electrodiagnostic medicine*, First. 1995.

[12] A. Fuglsang-Frederiksen, "The role of different EMG methods in evaluating myopathy", *Clinical Neurophysiology*, vol. 117, pp. 1173–1189, 2006.

[13] J. R. Daube and D. I. Rubin, "Needle electromyography", *Muscle and Nerve*, vol. 39, pp. 244–270, 2009.

[14] G. Drost, *High-density surface EMG pathophysiological insights and clinical applications*. 2013, p. 144.

[15] A. Holobar, D. Farina, M. Gazzoni, R. Merletti, and D. Zazula, "Estimating motor unit discharge patterns from high-density surface electromyogram", *Clinical Neurophysiology*, vol. 120, pp. 551–562, 2009.

[16] G. Drost, D. F. Stegeman, B. G. van Engelen, and M. J. Zwarts, "Clinical applications of high-density surface EMG: A systematic review", *Journal of Electromyography and Kinesiology*, vol. 16, pp. 586–602, 2006.

[17] R. Merletti and A. P. Parker, *Electromyography. Physiology, Engineering and Noninvasive Applications*. 2004.

[18] J. Y. Hogrel, "Clinical applications of surface electromyography in neuromuscular disorders", *Neurophysiologie Clinique*, vol. 35, no. 2-3, pp. 59–71, 2005.

[19] M. J. Zwarts and D. F. Stegeman, "Multichannel surface EMG: Basic aspects and clinical utility", *Muscle and Nerve*, vol. 28, no. 1, pp. 1–17, 2003.

[20] S. Paganoni and A. Amato, "Electrodiagnostic Evaluation of Myopathies", *Phys Med Rehabil Clin*, vol. 23, no. 1, pp. 193–207. 2013.

[21] K. R. Mills, "The basics of electromyography", *Neurology in Practice*, vol. 76, pp. 32–35, 2005.

[22] N. P. Young, J. R. Daube, E. J. Sorenson, and M. Milone, "Absent, unrecognized, and minimal myotonic discharges in myotonic dystrophy type 2", *Muscle and Nerve*, vol. 41, no. 6, pp. 758–762, 2010.

[23] A. Gallina and A. Botter, "Spatial localization of electromyographic amplitude distributions associated to the activation of dorsal forearm muscles", *Frontiers in Physiology*, 2013.

[24] M. Gazzoni, D. Farina, and R. Merletti, "A new method for the extraction and classification of single motor unit action potentials from surface EMG signals", *Journal of Neuroscience Methods*, vol. 136, no. 2, pp. 165–177, 2004.

[25] R. Merletti, A. Holobar, and D. Farina, "Analysis of motor units with high-density surface electromyography", *Journal of Electromyography and Kinesiology*, vol. 18, no. 6, pp. 879–890, 2008.

[26] M. Rojas-Martínez, M. A. Mañanas, and J. F. Alonso, "High-density surface EMG maps from upper-arm and forearm muscles", *Journal of NeuroEngineering and Rehabilitation*, vol. 9, no. 1, 2012.

[27] I. Gligorijević, B. T. Sleutjes, M. De Vos, J. H. Blok, I. Montfoort, B. Mijović, M. Signoretto, and S. Van Huffel, "Motor unit tracking using high density surface electromyography (HDsEMG): Automated correction of electrode displacement errors", *Methods of Information in Medicine*, vol. 54, no. 3, pp. 221–226, 2015.

[28] C. W. N. S. S. J. R. B. Usselman, "Motor Unit Number Estimation Based on High-Density Surface Electromyography Decomposition", *Physiology & behavior*, vol. 176, no. 3, pp. 139–148, 2017.

[29] C. Torres, R. T. Moxley, and R. C. Griggs, "Quantitative testing of handgrip strength, myotonia, and fatigue in myotonic dystrophy", *Journal of the Neurological Sciences*, vol. 60, no. 1, pp. 157–168, 1983.

[30] R. T. Moxley, E. L. Logigian, W. B. Martens, C. L. Annis, S. Pandya, R. T. Moxley IV, C. A. Barbieri, N. Dilek, A. W. Wiegner, and C. A. Thornton, "Computerized hand grip myometry reliably measures myotonia and muscle strength in myotonic dystrophy (DM1)", *Muscle and Nerve*, vol. 36, no. 3, pp. 320–328, 2007.

[31] L. A. Cotelez, M. V. G. B. Serra, E. Ramos, J. E. Zaia, F. O. Toledo, and P. R. V. Quemelo, "Handgrip strength and muscle fatigue among footwear industry workers", *Fisioterapia em Movimento*, vol. 29, no. 2, pp. 317–324, 2016.

[32] J. B. Pitcher and T. S. Miles, "Influence of muscle blood flow on fatigue during intermittent human hand-grip exercise and recovery", *Clinical and Experimental Pharmacology and Physiology*, vol. 24, no. 7, pp. 471–476, 1997.

[33] A. Merlo, D. Farina, and R. Merletti, "A fast and reliable technique for muscle activity detection from surface EMG signals", *IEEE Transactions on Biomedical Engineering*, vol. 50, no. 3, pp. 316–323, 2003.

[34] D. Farina, A. Holobar, R. Merletti, and R. M. Enoka, "Decoding the neural drive to muscles from the surface electromyogram", *Clinical Neurophysiology*, vol. 121, no. 10, pp. 1616–1623, 2010.

[35] A. Holobar and D. Zazula, "Multichannel blind source separation using convolution Kernel compensation", *IEEE Transactions on Signal Processing*, vol. 55, no. 9, pp. 4487–4496, 2007.

[36] B. Montmollin and W. Strahm, "Decomposition of Surface EMG Signals", vol. 96, pp. 1646–1657, 2006.

[37] A. Holobar, M. A. Minetto, and D. Farina, "Accurate identification of motor unit discharge patterns from high-density surface EMG and validation with a novel signal-based performance metric", *Journal of Neural Engineering*, vol. 11, no. 1, 2014.

[38] A. Holobar and D. Zazula, "Gradient convolution kernel compensation applied to surface electromyograms", *Lecture Notes in Computer Science (including subseries Lecture Notes in Artificial Intelligence and Lecture Notes in Bioinformatics)*, vol. 4666 LNCS, pp. 617–624, 2007.

[39] A. Holobar and D. Zazula, "Correlation-based decomposition of surface electromyograms at low contraction forces", *Medical and Biological Engineering and Computing*, vol. 42, no. 4, pp. 487–495, 2004.

[40] D. Zazula and E Plévin, "An approach to decomposition of muscle and nerve signals", *Int. Conf. on Signal, Speech, and Image Processing . . .*, pp. 1–6, 2002.

[41] E. L. Logigian, W. B. Martens, R. T. Moxley, M. P. McDermott, N. Dilek, A. W. Wiegner, A. T. Pearson, C. A. Barbieri, C. L. Annis, C. A. Thornton, and R. T. Moxley, "Mexiletine is an effective antimyotonia treatment in myotonic dystrophy type 1", *Neurology*, vol. 74, no. 18, pp. 1441–1448, 2010.